University Transportation Research Center - Region 2

Final Report

Investigation of the Carrs Creek Geofoam Project

Performing Organization: Syracuse University

August 2014

Sponsor:
University Transportaton Research Center - Region 2

University Transportation Research Center - Region 2

The Region 2 University Transportation Research Center (UTRC) is one of ten original University Transportation Centers established in 1987 by the U.S. Congress. These Centers were established with the recognition that transportation plays a key role in the nation's economy and the quality of life of its citizens. University faculty members provide a critical link in resolving our national and regional transportation problems while training the professionals who address our transportation systems and their customers on a daily basis.

The UTRC was established in order to support research, education and the transfer of technology in the field of transportation. The theme of the Center is "Planning and Managing Regional Transportation Systems in a Changing World." Presently, under the direction of Dr. Camille Kamga, the UTRC represents USDOT Region II, including New York, New Jersey, Puerto Rico and the U.S. Virgin Islands. Functioning as a consortium of twelve major Universities throughout the region, UTRC is located at the CUNY Institute for Transportation Systems at The City College of New York, the lead institution of the consortium. The Center, through its consortium, an Agency-Industry Council and its Director and Staff, supports research, education, and technology transfer under its theme. UTRC's three main goals are:

Research

The research program objectives are (1) to develop a theme based transportation research program that is responsive to the needs of regional transportation organizations and stakeholders, and (2) to conduct that program in cooperation with the partners. The program includes both studies that are identified with research partners of projects targeted to the theme, and targeted, short-term projects. The program develops competitive proposals, which are evaluated to insure the mostresponsive UTRC team conducts the work. The research program is responsive to the UTRC theme: "Planning and Managing Regional Transportation Systems in a Changing World." The complex transportation system of transit and infrastructure, and the rapidly changing environment impacts the nation's largest city and metropolitan area. The New York/New Jersey Metropolitan has over 19 million people, 600,000 businesses and 9 million workers. The Region's intermodal and multimodal systems must serve all customers and stakeholders within the region and globally.Under the current grant, the new research projects and the ongoing research projects concentrate the program efforts on the categories of Transportation Systems Performance and Information Infrastructure to provide needed services to the New Jersey Department of Transportation, New York City Department of Transportation, New York Metropolitan Transportation Council , New York State Department of Transportation, and the New York State Energy and Research Development Authorityand others, all while enhancing the center's theme.

Education and Workforce Development

The modern professional must combine the technical skills of engineering and planning with knowledge of economics, environmental science, management, finance, and law as well as negotiation skills, psychology and sociology. And, she/he must be computer literate, wired to the web, and knowledgeable about advances in information technology. UTRC's education and training efforts provide a multidisciplinary program of course work and experiential learning to train students and provide advanced training or retraining of practitioners to plan and manage regional transportation systems. UTRC must meet the need to educate the undergraduate and graduate student with a foundation of transportation fundamentals that allows for solving complex problems in a world much more dynamic than even a decade ago. Simultaneously, the demand for continuing education is growing – either because of professional license requirements or because the workplace demands it – and provides the opportunity to combine State of Practice education with tailored ways of delivering content.

Technology Transfer

UTRC's Technology Transfer Program goes beyond what might be considered "traditional" technology transfer activities. Its main objectives are (1) to increase the awareness and level of information concerning transportation issues facing Region 2; (2) to improve the knowledge base and approach to problem solving of the region's transportation workforce, from those operating the systems to those at the most senior level of managing the system; and by doing so, to improve the overall professional capability of the transportation workforce; (3) to stimulate discussion and debate concerning the integration of new technologies into our culture, our work and our transportation systems; (4) to provide the more traditional but extremely important job of disseminating research and project reports, studies, analysis and use of tools to the education, research and practicing community both nationally and internationally; and (5) to provide unbiased information and testimony to decision-makers concerning regional transportation issues consistent with the UTRC theme.

UTRC-RF Project No: 49997-48-24

Project Date: August 2014

Project Title: Investigation of the Carrs Creek Geofoam Project

Project's Website:
http://www.utrc2.org/research/projects/investigation-carrs-creek-geofoam-project

Principal Investigator:

Dr. Dawit Negussey
Professor
Program Director
Civil Engineering, Geofoam Research Center
Syracuse University
151 Link Hall
Syracuse, NY 13244
Email: negussey@syr.edu

Research Participatns:

Graduate students:
- *Amsalu Birhan*
- *Chen Liu*
- *Stephen Singh*

Undergraduate student:
- *Luka Andrews*

Performing Organizations: Geofoam Research Center - Syracuse University

Sponsor:

University Transportation Research Center - Region 2, A Regional University Transportation Center sponsored by the U.S. Department of Transportation's Research and Innovative Technology Administration

To request a hard copy of our final reports, please send us an email at utrc@utrc2.org

Mailing Address:

University Transportation Reserch Center
The City College of New York
Marshak Hall, Suite 910
160 Convent Avenue
New York, NY 10031
Tel: 212-650-8051
Fax: 212-650-8374
Web: www.utrc2.org

Board of Directors

The UTRC Board of Directors consists of one or two members from each Consortium school (each school receives two votes regardless of the number of representatives on the board). The Center Director is an ex-officio member of the Board and The Center management team serves as staff to the Board.

City University of New York
Dr. Hongmian Gong - Geography
Dr. Neville A. Parker - Civil Engineering

Clarkson University
Dr. Kerop D. Janoyan - Civil Engineering

Columbia University
Dr. Raimondo Betti - Civil Engineering
Dr. Elliott Sclar - Urban and Regional Planning

Cornell University
Dr. Huaizhu (Oliver) Gao - Civil Engineering
Dr. Mark A. Turnquist - Civil Engineering

Hofstra University
Dr. Jean-Paul Rodrigue - Global Studies and Geography

Manhattan College
Dr. Anirban De - Civil & Environmental Engineering
Dominic Esposito - Research Administration

New Jersey Institute of Technology
Dr. Steven Chien - Civil Engineering
Dr. Joyoung Lee - Civil & Environmental Engineering

New York Institute of Technology
Dr. Nada Marie Anid - Engineering & Computing Sciences
Dr. Marta Panero - Engineering & Computing Sciences

New York University
Dr. Mitchell L. Moss - Urban Policy and Planning
Dr. Rae Zimmerman - Planning and Public Administration

Polytechnic Institute of NYU
Dr. John C. Falcocchio - Civil Engineering
Dr. Kaan Ozbay - Civil Engineering

Rensselaer Polytechnic Institute
Dr. José Holguín-Veras - Civil Engineering
Dr. William "Al" Wallace - Systems Engineering

Rochester Institute of Technology
Dr. J. Scott Hawker - Software Engineering
Dr. James Winebrake -Science, Technology, & Society/Public Policy

Rowan University
Dr. Yusuf Mehta - Civil Engineering
Dr. Beena Sukumaran - Civil Engineering

Rutgers University
Dr. Robert Noland - Planning and Public Policy

State University of New York
Michael M. Fancher - Nanoscience
Dr. Catherine T. Lawson - City & Regional Planning
Dr. Adel W. Sadek - Transportation Systems Engineering
Dr. Shmuel Yahalom - Economics

Stevens Institute of Technology
Dr. Sophia Hassiotis - Civil Engineering
Dr. Thomas H. Wakeman III - Civil Engineering

Syracuse University
Dr. Riyad S. Aboutaha - Civil Engineering
Dr. O. Sam Salem - Construction Engineering and Management

The College of New Jersey
Dr. Thomas M. Brennan Jr. - Civil Engineering

University of Puerto Rico - Mayagüez
Dr. Ismael Pagán-Trinidad - Civil Engineering
Dr. Didier M. Valdés-Díaz - Civil Engineering

UTRC Consortium Universities

The following universities/colleges are members of the UTRC consortium.

City University of New York (CUNY)
Clarkson University (Clarkson)
Columbia University (Columbia)
Cornell University (Cornell)
Hofstra University (Hofstra)
Manhattan College
New Jersey Institute of Technology (NJIT)
New York Institute of Technology (NYIT)
New York University (NYU)
Polytechnic Institute of NYU (Poly)
Rensselaer Polytechnic Institute (RPI)
Rochester Institute of Technology (RIT)
Rowan University (Rowan)
Rutgers University (Rutgers)*
State University of New York (SUNY)
Stevens Institute of Technology (Stevens)
Syracuse University (SU)
The College of New Jersey (TCNJ)
University of Puerto Rico - Mayagüez (UPRM)

** Member under SAFETEA-LU Legislation*

UTRC Key Staff

Dr. Camille Kamga: *Director, UTRC*
Assistant Professor of Civil Engineering, CCNY

Dr. Robert E. Paaswell: *Director Emeritus of UTRC and Distinguished* Professor of Civil Engineering, The City College of New York

Herbert Levinson: *UTRC Icon Mentor, Transportation Consultant and Professor Emeritus of Transportation*

Dr. Ellen Thorson: *Senior Research Fellow, University Transportation Research Center*

Penny Eickemeyer: *Associate Director for Research, UTRC*

Dr. Alison Conway: *Associate Director for New Initiatives and Assistant Professor of Civil Engineering*

Nadia Aslam: *Assistant Director for Technology Transfer*

Dr. Anil Yazici: *Post-doc/ Senior Researcher*

Nathalie Martinez: *Research Associate/Budget Analyst*

TECHNICAL REPORT STANDARD TITLE PAGE

1. Report No.	2.Government Accession No.	3. Recipient's Catalog No.

4. Title and Subtitle	5. Report Date
Investigation of the I88 Carrs Creek Geofoam Failure	August 20, 2014
	6. Performing Organization Code

7. Author(s)	8. Performing Organization Report No.
Dawit Negussey, Stephen Singh, Luke Andrews, Chen Liu, Amsalu Birhan	

9. Performing Organization Name and Address	10. Work Unit No.
Geofoam Research Center - Syracuse University, 151 Link Hall, Syracuse, NY, 13244-1240	11. Contract or Grant No. 49997-48-24

12. Sponsoring Agency Name and Address	13. Type of Report and Period Covered
Research and Innovative Technology Administration U.S. Department of Transportation 1200 New Jersey Avenue, Washington, DC 20590	Final Report 14. Sponsoring Agency Code

15. Supplementary Notes

16. Abstract

The I88 culvert crossing of Carrs Creek in Sidney, NY collapsed during the record setting Mid-Atlantic States Flood of June 2006. Rapid construction with geofoam as lightweight fill enabled partial reopening of I88 by Labor Day 2006. Shortly after reopening of the roadway, rapid settlements developed. The geofoam fill was removed and I88 was re-built using lightweight aggregates. An investigation of the rapid construction failure was completed in 2009. This report examines the failure of the re-construction and the results of the subsequent investigation. Alternative causes for the failure have been identified based on previous observations, lab tests and computer models. Suggestions for improving rapid construction practice with geofoam are provided.

17. Key Words	18. Distribution Statement
Culvert, failure, flood, geofoam, rapid construction, creep, settlement	

19. Security Classif (of this report)	20. Security Classif. (of this page)	21. No of Pages	22. Price
Unclassified	Unclassified	53	

Form DOT F 1700.7 (8-69)

Project Title: Investigation of the I88 Carrs Creek Geofoam Failure

University: Geofoam Research Center - Syracuse University

Principal Investigator: Dawit Negussey

Research Participants:

Graduate students:

Amsalu Birhan

Chen Liu

Stephen Singh

Undergraduate student:

Luke Andrews

Sponsors: US DOT Region 2 University Transportation Research Center

Completion Date: August 2014

Disclaimer

Executive Summary

The I88 culvert crossing of Carrs Creek in Sidney, NY collapsed during the record setting Mid-Atlantic States Flood of June 2006. Rapid construction with geofoam as lightweight fill enabled partial reopening of I88 by Labor Day 2006. Shortly after reopening of the roadway, rapid settlements developed. The geofoam fill was removed and I88 was re-built using lightweight aggregates. An investigation of the rapid construction failure was completed in 2009. This report examines the re-construction failure through lab tests, computer models and review of the previous investigation. Possible causes for the failure were identified and an alternative design with geofoam is presented. The following are the main conclusions and suggestions for improving rapid construction practice with geofoam.

Excessive deformation of geofoam was likely caused by the following factors:

- More than 30% of the geofoam blocks were of lower than acceptable density.
- The compacted earth fill and overlying pavement imposed excessive pressures.
- Lack of internal drainage and directed runoff produced increased loading.
- Continuous rather than staggered vertical joints were less effective in promoting integral response of the geofoam fill.
- Heavy axle loads and compaction in wet conditions directly above the geofoam surface, without benefit of a load distribution slab, likely damaged geofoam blocks in the top layer.
- Interactions between blocks of different densities led to overstressed zones and localized creep deformations.
- The vertical interface between the compacted soil and geofoam blocks facilitated higher lateral pressures and greater creep deformations.

The following suggestions are provided to improve rapid construction practice using geofoam:

- Limit vertical pressures from dead and live loads to less than 50% of the unconfined compression strength at 10% strain or stress at 1% strain, whichever is less.
- Avoid continuous vertical joints between successive geofoam layers.
- Provide a stepped transition between soil and geofoam interfaces placing geofoam blocks on top and not below compacted soil.
- Request the manufacturer to provide in plant quality control data for all supplied blocks and also weigh blocks to accept or reject on delivery or implement a robust quality assurance program.
- Require full size blocks to meet the specified density as a minimum and not exceed the specified density by more than 10%.
- Specify full lengths (16ft) rather than half lengths (8ft) blocks unless necessary to form specific shapes or edges.
- Provide base and side internal drainage and direct surface flow away from the geofoam fill area to prevent submersion of blocks and high groundwater levels.
- Use a load distribution slab over geofoam surfaces below road lanes or consider installing geogrids to attenuate stress increments from compaction during construction.
- Consider stockpiling geofoam blocks and pre-cast load distribution slab segments as rolling stock for regular projects and for emergency construction.

Table of Contents

List of Figures

List of Tables

Introduction

This report presents background on the failure of a rapid re-construction of the I88 culvert crossing of Carrs Creek that collapsed in 2006 and the investigation of the failed re-construction that followed (1). Field information, test results and conclusions presented in the previous report are re-examined. This investigation includes re-assessment of the field data, review of test results and attributed causes for the failure through computer modeling and alternative laboratory tests to reach different conclusions. Lessons learned from the failure and insights gained from the investigation are used to provide an alternative design. Suggestions to improve rapid *construction practice with geofoam are provided.*

Background

The I88 culvert at Carrs Creek in Sidney, NY; collapsed during the record Mid-Atlantic States Flood in June 2006 (2). The failure is about 56km (35 miles) northeast of Binghamton (Figure 1). The 9.1m (30ft) wide corrugated metal plate culvert was built in 1974 and had received a rating of 5 out of 7 in the bi-annual NYSDOT survey of 2004. The rating of 5 represents minor deterioration but was otherwise of acceptable structural and functional grade (3). By the early morning of June 28, the Carrs Creek flood stage rose above the inlet and the culvert collapsed (Fig 2). A truck heading east and another traveling west fell into the wide trench formed by the culvert failure and washout of the roadway. Both drivers lost their lives. The I88 section between Sidney and Unadilla, NY was closed. Delaware County was declared a Federal Disaster Area. Labor Day 2006 was established as the target date for rapid construction and reopening of I88.

Reconstruction

The reconstruction design is shown in plan, section and elevation in Figures 3, 4 and 5 from the previous investigation (1). The reconstruction featured a segmental 3 sided precast concrete culvert on H pile foundation. A standard pre-cast concrete section of 12.8m (42ft) clear span was selected but the required cover of up to 6.4m (21ft) was considered too high. Custom made pre-cast concrete culvert segments could not be produced within the proposed construction timeline. Lightweight aggregates, lightweight concrete and geofoam were considered to reduce the overburden pressure on the culvert to acceptable levels. EPS geofoam of 0.2kN/m^3 (1.25pcf) nominal density was selected. The project material specification required random weighing of one block per truck load on delivery for quality assurance. Any block in a truck load failing to meet the nominal density criteria was cause to reject the entire truck load. EPS geofoam was ordered on August 8 and delivery of 819 blocks began two days later. Installation of 0.9X1.2X2.4m (3X4X8ft) geofoam blocks began on August 21 and was completed within three days. Geofoam blocks were placed on soil bedding over the culvert, in 3 layers for 2.7m (9ft) on the eastbound and 2 layers for 1.8m (6ft) height on the westbound. As specified, the orientation of block axes in successive layers was rotated. However, the installation featured continuous vertical joints at 2.4m (8ft) spacing in transverse and longitudinal directions (Figure 7). This resulted in separate columns of 2.4m by 2.4m (8ft by 8ft) dimensions in plan. Due to the urgency of the construction and to meet the target opening date, a cast in place reinforced concrete load distribution slab on the geofoam top surface was not provided. Instead, the top surface and edge overhang on the perimeter of the geofoam fill were covered with a geomembrane barrier. The relatively large depth of burial of 2.4m (8ft) on westbound and 3.4m (11ft) on eastbound was intended to

attenuate stress increments on the geofoam from heavy axle loads. The geofoam / compacted soil separation above the culvert side walls was vertical (Figure 8) rather than stepped as in previous soil/geofoam interface transitions. The soil fill adjacent and above the geofoam installation was compacted in wet conditions. Paving of the westbound lanes was completed by Labor Day and I88 was opened for restricted two way traffic, while work on the eastbound lanes continued (1).

Settlements

Settlement of the westbound asphalt surface and transverse cracks along the eastbound compacted fill became evident shortly after I88 westbound opened for two way traffic. The underlying pre-cast concrete culvert showed no evidence of distress. Settlement observations at westbound Station 2+913 started shortly after completion of paving. Initially rapid settlements slowed and gradually reached an accumulated total movement of about 30cm after 10 months (Figure 9). Much of the initial settlement of the geofoam below the eastbound roadway was not recorded. This is reflected in the slower rate of initial settlement observations for the eastbound at Station 2+904). A total of about 45cm settlement developed in only 4 months. The settlement profile of the eastbound embankment across the culvert also showed initially rapid change and then slowed (Figure 10). Trucks passing over the culvert produced bouncing movements (1). Settlements of the compacted soil adjacent to the geofoam and above the culvert sides were relatively negligible. Paving of the eastbound roadway was delayed after placement of the compacted soil.

Supplementary laboratory tests were performed on 2 fresh blocks provided by the supplier and tube samples recovered from 2 drill holes near the culvert centerline and along the middle of the eastbound embankment. Consolidation under 72kPa (1500psf) pressure as equivalent to 3.4m (11ft) of fill produced 21 to 41 percent strain after 2 to 7 days of loading. Two block samples were trimmed from blocks WB-B-15A-2 and WB-B-15B-1 along the north facing side slope of the westbound roadway. The same consolidation load applied over 126 days on a sample from WB-B15A-2 produced 30% strain. The 72kPa (1500psf) pressure is about 65% of the strength at 10% strain for the specified geofoam and a higher percentage for geofoam blocks of lower density. The responses of geofoam in constrained and unconfined compression were noted to be essentially identical (4). The large deformations that developed under sustained loading are consistent with previous results (5, 6) for 70% of strength at 10% strain loading on the same geofoam density grade over 2 years. Average densities and strengths for fresh block 1, and recovered blocks WB-B-15A-2 and WB-B-15B-1 were below values for EPS19 in ASTM D 6817, the specified grade geofoam. Densities and strengths at 10% strain for the pre-stressed tube samples met the ASTM D 6817 criteria for EPS19 and the project specification. Two independent laboratories participated in this first round of pre-removal testing. Isolated detection of the geofoam top and base movements with expanding anchor Borros points identified the geofoam fill as the primary cause for the deformations observed at surface. Feedback and technical guidance from FHWA and industry sources (1) were unclear. A decision was made to remove and replace the geofoam and overlying compacted soil with lightweight aggregates.

Removal

On removal of the pavement and compacted soil, the geomembrane barrier over the surface of the geofoam became exposed. The geofoam top surface was sloped towards the roadway and culvert centerlines as a bowl shaped depression. Blocks uncovered from under low fill heights along the side slopes were less deformed than blocks below high fills under the roadway (Figures 11 and 12). There was perched water in the bowl shape above the geomembrane and pooling below the geofoam and above the culvert surface (Figures 13 and 14). As the geomembrane cover was removed, the exposed geofoam top surface and side overhang were clean (Figure 15). The location, weight and dimensions of 177 blocks were recorded following a labeling convention (Figure 16). A subset of 48 blocks were again weighed and measured after drying. These 48 blocks were stored in a warehouse for further testing and evaluation. Table 1 is a summary of exhumed block weights and dimensions. Two blocks, one from the top layer of the eastbound (EB-T-7D1) and the other from the bottom layer of the westbound (WB-B-9B3) were selected for detailed testing. All other blocks were moved to a storage yard (Figure 17).

Further Tests

Samples from exhumed blocks EB-T-7D1 and WB-B-9B3 were tested in four independent laboratories (1). Based on over 100 density and unconfined compression tests, in accordance with ASTM D 1621 and 1622, the exhumed blocks met requirements of the project specification. However, the results indicated the strengths at 1% strain were lower than values provided for EPS19 in ASTM D 6817. The strengths at both the 5% and 10% strain were accepted to be in conformance with the ASTM standard. The NYSDOT specification did not have a 1% strain

criterion. The investigation concluded the low strengths at 1% strain, possibly due to high regrind or recycled content, caused the poor performance of the geofoam and settlements of the roadway. NYSDOT accordingly revised the EPS geofoam material specification to include a strength criterion at 1% strain (1).

Re-Investigations

The record of exhumed block locations and measurements were used to develop settlement profiles and to examine the density range of the installed geofoam blocks. The information on exhumed blocks was also helpful to compare the two blocked selected for round robin testing with other exhumed blocks. Precipitation data from weather stations in Sidney (about 3 miles) and Unadilla (about 1.5 miles from the site) were reviewed to identify occurrences of intense rainfall during and after construction (Figure 18). Computer model simulations were developed to represent the compacted soil, geofoam and pre-stressed concrete culvert interactions. Stress conditions indicated by computer models were applied to laboratory samples to develop further understanding of the geofoam response and installation effects. Constitutive relations were modified to incorporate the laboratory findings. Small block models were tested to examine effects of mixed geofoam densities and joint patterns.

Review of Records

Using the layer plans and nominal block dimensions, the 3D model of the geofoam installation was developed (Figure 19). The locations of exhumed blocks within the 3D model are as shown. Also shown are locations of 29% of exhumed blocks that weighed below 90% of the weight for the specified nominal density. In some locations inferior grade blocks were stacked in the same

2.4 by 2.4m (8 by 8ft) column. The average deformation and location of exhumed blocks for the eastbound and westbound sections along the culvert centerline are shown in Figures 20 and 21. The deformation profiles are concave upward as was the exposed geofoam surface. The largest geofoam block deformations were below the highest fill zones under the roadways. A ranking of the top 25 of the largest block deformations shows that the top 72% and 84% of the ranked group were below the 3.4m (11ft) high fill of the eastbound embankment (Figure 22). The lack of sensible correlation between large deformation magnitudes and low block densities suggests interaction effects between blocks of different densities. This is also evident in the plot of average strains and block weights where values for EB-T-7D1 and WB-B-9B3 are also shown (Fig 23). These two blocks were selected for round robin testing but were among the least deformed and of better density than many other exhumed blocks. The number of lower grade blocks would have been higher with adjustment for weight increase due to wetting, as shown. The adjustment estimate was based on 1 week emersion tests and allowance for surface area to volume ratio of the block dimensions. Blocks of lower weight, such as WB-B-15A-2 and WB-B-15B-1 tested in the supplementary test program before removal, did not meet both the density and strength values for EPS19 in ASTM D 6817. However, the cause of failure was only attributed to low strengths at 1% strain observed in the round robin test program after removal. Precipitation records from weather stations closest to the site from 3 days before the start of geofoam installation and continuing through the post construction period are shown in Figure 24. As indicated in the previous investigation report, compaction occurred under very wet conditions. Saturation of the fill and ponding of surface runoff increased total pressures on the geofoam blocks and the potential for more creep strains, as will be discussed under lab tests below.

Computer Models

The eastbound and westbound sections of culvert crossings were modeled in FLAC (7) to examine internal stress distributions. Relying on symmetry, only half of the geofoam fill was represented, as shown for the eastbound lanes (Figure 25). The geofoam was represented as an elastic material with 4MPa (0.58ksi) modulus. Material properties for the compacted soil and pavement are provided in Table 2. The vertical pressure profiles along the base of the geofoam across the east and, westbound lanes and the lowest level of the median are shown in Figure 26. The width of the sections extend to reach free field conditions for the embankment loading. The free field stress for the eastbound was highest because of the largest thickness of compacted soil cover. Vertical stresses at the base of the geofoam were highest at the centerline and decreased above the culvert wall. Within the relatively stiffer compacted soil adjacent to the geofoam, vertical stresses increased above the free field levels due to arching. The vertical pressure profile for both the east and west bound directions were consistent with the profile of the geofoam top surface observed in the field and also suggested by the deformation profile of exhumed blocks in Figures 11 and 12. The vertical stress profile along the top and base of the geofoam fill were approximately the same because the geofoam weight was relatively insignificant. The maximum vertical stress of 75kPa (1.6ksf) in the eastbound geofoam represents a 45% reduction from the free field condition for the compacted fill along the geofoam base and 68% of the strength at 10% strain for the specified density geofoam. While the 45% reduction of load on the culvert by geofoam substitution was very significant and beneficial, the 68% of strength load supported by the geofoam was too high and should have been of concern. Because of the depth of burial and vertical interface between the geofoam and compacted soil; the FLAC models indicated lateral

pressures of up to 30kPa (627psf) likely developed at the geofoam and compacted soil vertical interface (Figure 27). Inundation of the median after intense rainstorms further increased both the vertical and lateral total pressures on the geofoam blocks for limited durations. More results from the FLAC simulations are reported in (8).

Lab tests

Laboratory tests were performed on fresh samples provided by the geofoam supplier and also on exhumed blocks retrieved from field storage. The tests aimed to examine influences of pre-strain on initial modulus, effects of confining pressure on geofoam strength and creep behavior as well as to compare these results with standard unconfined compression results. Additional tests were performed to observe undrained cyclic loading behavior of geofoam samples.

Figure 28 shows unconfined compression loading and re-loading after large pre-strain of a virgin sample. The initial modulus in virgin loading was over three times greater than the modulus for re-loading. Figure 29 shows unconfined compression results for pre-strained samples cut from highly compressed exhumed blocks. The results indicate the initial moduli for loading in the pre-strained direction were much lower than for samples loaded in directions transverse to the pre-strain and for virgin loading conditions. Reduction of initial moduli increase with the level of pre-strain or pre-loading (9). The density of pre-strained samples were significantly increased by the permanent pre-strain (Table 3). Blocks EB-T-7D1 and WB-B-9B3 indicated pre-strain of 2.5 to 7.5% in height, based on measured dimensions when exhumed. With allowance for rebounding, the pre-strain would have been greater than was inferred from measurements after recovery. The observation of inferior strengths at 1% strain but acceptable density and strengths at 10%

strain in the previous study can be attributed to induced anisotropy caused by prior loading beyond yield.

Both test blocks were of about equal weight and close to the lower bound of acceptable densities. The pre-straining effect would tend to exaggerate the density estimates of test specimens. The volume of geofoam produced within a short time was large. Adequate supply of regrind from plant operations was unlikely to be available to affect the recycled content to an extent that would have affected 1% level performance. Manufacturers do not add regrind from sources outside the plant. If representative samples from the full range of block weights were included in the multi laboratory test program, low strengths at 1, 5 and 10% strain would have been easily observed for substandard low density blocks.

The poor performance of geofoam blocks was re-assessed in terms of unconfined compression test results on exhumed samples. Yet, because of the deep burial, continuous vertical interface between geofoam blocks and the compacted soil side fill as well as periodic high groundwater levels; the geofoam blocks were subjected to confined compression. Results of unconfined and confined compression at different constant cell pressure levels on cylindrical geofoam samples are shown in Figure 30. The results show that strengths at 1, 5 and 10% strain reduced significantly as confining pressures increased, as was also reported previously (10, 11,12). Figure 31 shows more creep strains developed at the same deviator stress level but with increasing confining pressures (13).

Cyclic cell pressures and deviator stresses were applied to cylindrical geofoam samples within triaxial cells. The results shown in Figure 32 represent initial confining pressure followed by cycles

of deviator stress or cyclic cell pressure. The cyclic load increments caused cyclic deformations and accumulating strains. The bouncing movements of the roadway surface with passage of heavy trucks may have been associated with dynamic pore pressure changes during high groundwater conditions, as in the cyclic load response. The compacted soil surrounding the top and sides of the geofoam fill was not free draining. Other than a thin geo-composite drain interface along the culvert side walls and 1.8m (6ft) below the geofoam base, there was no internal drainage system. An additional contributing factor for development of high groundwater levels was drainage of surface runoff towards the culvert from both the east and west sides of the median.

Lab Tests on Multiple Blocks

To examine the effects of mixed densities and connected vertical gaps, compression tests were performed on two layers of stacked small size blocks. In the first test, six 50mm (2in) cube samples were stacked in 2 layers of three blocks maintaining continuous vertical gaps. All 6 samples were of the specified 0.2kN/m^3 (1.5pcf) density in one test and of the specified and lower grade 0.16kN/m^3 (1pcf) density combinations in the top and lower layers in a second test (Figure 33). All samples deformed about equally when the densities were all the same and the interface between the upper and lower blocks remained horizontal. In the mixed density test, lower density blocks deformed more than the specified blocks and the initially horizontal interface between the layers became uneven. Strengths at 1, 5 and 10% strain for the uniform density set were higher than corresponding strengths for the mixed density set. In repeat tests the three top layer 50mm (2in) cubes were replaced with two 75mm (3in) wide blocks (Figure 34). For these tests with two upper and three lower blocks, the vertical joints were staggered and not

continuous as required in the specification. The 5 blocks of the specified density deformed uniformly and the interface between the upper and lower blocks remained horizontal as well. For the 5 blocks of mixed density, blocks of low density deformed more than the blocks of the specified density. The interface between the upper and lower blocks was uneven but was less so than for the 6 block layers with continuous joints. Strengths at 1, 5 and 10% for the 5 blocks mixed density set were slightly higher than for 6 blocks mixed density. The test results indicate both density differences and continuous vertical joints degrade the strength and deformation performance.

The unconfined compression loading of the 5 and 6 blocks by rigid end plates imposed uniform displacement along the platen interfaces. FLAC models of the rigid boundary and constant displacement rate conditions also indicated uniform displacement but non uniform boundary pressures. In the field, the top surface of the geofoam was unevenly deformed locally and with transverse and longitudinal concave up curvature globally. The field mixed boundary conditions were simulated in FLAC models of the lab tests, both with and without interface elements in vertical gaps, and uniform pressure of 75kPa (1566psf) on the top boundary. The mixed boundary conditions results, as in the field, are shown in Figure 35. Blocks of higher density carried more load and blocks of lower density deformed more. The top surface of the FLAC models indicate uneven deformations as observed in the field. High differential pressures that exceed the pressure applied at the top boundary developed in portions of dense blocks adjacent to low density blocks (Figure 36). For the 5 blocks with staggered joints, the portion of the weak block and underlying low density blocks deformed more than the higher density blocks (Figure 37). Stresses of more than double the applied pressure at the top boundary developed in portions of

the dense blocks (Figure 38). Hence the non-uniformity in density contributed to development of internal pressures that exceeded presumed allowable levels for the specified geofoam grade. Thus depending on the densities of surrounding blocks, edges of individual blocks deformed unequally as occurred in the field. The maximum, average and minimum heights for acceptable and below grade blocks were about the same (Table 1). This may be due to interaction effects and higher density blocks supporting more load.

Simulating Field Settlements

The observed surface settlement profile of the eastbound roadway at three different times are shown in Figure 39 with computed settlements using different initial moduli and an exponential stress strain relation (9) to represent both unconfined and confined stress states. The material properties used in the FLAC simulations are given in Table 2. The first modulus of 6MPa (0.87ksi) for fitting the lowest deformation level on 11/7/06 is higher than 4MPa (0.58ksi) listed in ASTM D 6817 for EPS19. The initial modulus of the much larger actual blocks was higher than values from lab tests on small samples as was also observed in previous field (14) and laboratory (15) studies. The second and third set of moduli of 0.55MPa (0.08ksi) and 0.375MPa (0.05ksi) are much lower than the moduli from the round robin testing and account for the combination of creep, confining pressures, mixed densities and continuous joints over time. Settlements predicted by using an equivalent modulus of 3MPa (0.44ksi) and unconfined compression, as implied by the results of the previous study (1), predict maximum settlements of the order of only 50mm (2in). Whereas, the actual settlements were of the order of 10 times greater. Confining pressures, creep, mixed densities and continuous joints likely played a part in producing the large post re-construction settlements of I88.

Conclusions

Review of field observations, results of lab tests and computer models suggest poor performance of EPS geofoam for the emergency reconstruction of the I88 culvert at Carrs Creek was likely caused by a culmination of the following factors:

- More than 30% of the geofoam blocks were of lower than acceptable density.
- The compacted earth fill and overlying pavement imposed excessive pressures.
- Lack of internal drainage and directed runoff produced increased loading.
- Continuous rather than staggered vertical joints were less effective in promoting integral response of the geofoam fill.
- Heavy axle loads and compaction in wet conditions directly above the geofoam surface, without benefit of a load distribution slab, likely damaged geofoam blocks in the top layer.
- Interactions between blocks of different densities led to overstressed zones and localized creep deformations.
- The vertical interface between the compacted soil and geofoam blocks facilitated higher lateral pressures and greater creep deformations.

In Hind Sight

The as built section in Figure 4 and an alternate design are shown in the longitudinal profile of geofoam and fill above the culvert centerline in Figure 40. Also shown are revised sections along

the eastbound and westbound roadways in Figures 41 and 42. By reducing the fill height above the geofoam and adding an additional layer of geofoam for the eastbound, the maximum vertical pressure has been reduced from 75kPa (1566psf) to 36kPa (752psf) or 33% of the unconfined compressive strength at 10% strain of EPS19 for all four sections in Figure 43. The median surface elevation has been raised and the geofoam transition from eastbound to westbound has more steps so as to direct runoff away from the geofoam area and to provide approximately even loading across the entire culvert profile. The vertical interface between the geofoam and the compacted soil has been stepped to reduce confining lateral pressures on the geofoam, Figure 44. The raised geofoam bedding above the culvert is free draining granular fill with perforated drain pipes along the lowest points above the culvert sidewalls. The granular bedding and drainage pipes would discharge by the culvert outlet. The free draining fill is separated from the compacted soil by geotextile filter. For the proposed alternative section, the geofoam surface below the roadways is capped with a mesh reinforced, poured in place or pre-cast, concrete load distribution slab. For good long term pavement performance and protection of geofoam blocks from compaction induced stresses during construction, use of concrete load distribution slab has worked well in previous NYS projects. As shown in Figure 45, a load distribution slab can significantly attenuate heavy compaction related stress increments during construction so as to limit damage and performance degradation while in service. The geofoam surface below soil within the median can be covered with geotextile or the geotextile can be omitted. The Susquehanna River flood stage to the north did not reach the culvert outlet during the 2006 record storm. Noting the destructive 2006 flood stage, probably as a 100 year design flood (2), at

the inlet; the geofoam fill along the length of the culvert can be checked for adequate resistance to uplift, if any.

Comparison of pressure profiles from FLAC models indicate vertical and confining stresses of 36kPa (752psf) and 22kPa (459psf) in the geofoam for the revised section (Table 4). Confining earth pressures are reduced and the drainage system dissipates hydrostatic pressures so that the strength of the geofoam fill can be reasonably represented by unconfined compression results. Where significant confining pressures remain, reduction factors can be used to adjust allowable pressures (8). For the as built eastbound profile with biaxial loading, mixed densities and hydrostatic pressures; vertical and confining pressures of up to 160kPa (3342psf) and 70kPa (1462psf) may have developed in the geofoam. Creep deformations that developed from these loads were well over 10% strain. Whereas, relatively small deformations for the alternative sections can be compensated by allowing the fill to stabilize before paving.

The purpose of using geofoam as light weight fill was to reduce the loading on the culvert. Because of the elliptic shape of the culvert roof, the edge of the culvert supports an additional 1.5m (5ft) of fill. Table 5 is a summary of load levels at the eastbound culvert center and side wall. The free field geostatic conditions represent pressure from soil fill without effect of arching. Assuming the pile supported culvert to be more rigid and settling less than the compacted soil of the side fill, negative arching develops to considerably increase the loading on the culvert side wall from about 174kPa (3.6ksf) to 270kPa (5.6ksf). The loading at the center is far removed from the culvert edge and would not be affected by arching. Replacement of the 2.7m (9ft) of soil fill with geofoam reduced the loading at the culvert center from 141kPa (2.9ksf) to 84kPa (1.8ksf).

The compacted soil side fill would be stiffer than the geofoam and soil fill over the culvert. Consequently, the loading above the culvert edge reduced from 270kPa (5.9ksf) to 140kPa (2.9ksf) by transferring the negative arching from above the culvert to the compacted soil side fill. For both the free field and negative arching conditions, rising water levels within the overlying fill would impose more load on the culvert. In the revised or alternate design section, adding an additional layer of geofoam reduced the loading at the culvert center from 84kPa (1.8ksf) to 67kPa (1.4ksf) and at the culvert edge from 140kPa (2.9ksf) to 135kPa (2.8ksf). However, the ratio of center of culvert to edge of culvert loading is 60% for the as built and 50% for the revised design. This is because the height of fill above the end of the culvert is increased from 1.8m (6ft) to 2.7m (9ft). As a result, more of the negative arching effect on the side fill spreads over towards the culvert edge in the revised design. The load at the end of the culvert can be further reduced by providing an additional layer of geofoam over the half width of the culvert section. Comparisons of major stresses on the culvert and the geofoam for the eastbound section are shown in Figure 46. The beneficial arching effect that developed with the geofoam fill may not be present with the light weight aggregate replacement. If the compacted lightweight aggregates deform less than the compacted soil, the dead load along the edge of the culvert wall may be more than anticipated due to negative arching.

Good performance of the geofoam fill will also require quality assurance for the supplied blocks and proper installation as per the specification. Mixing high and low density blocks can be detrimental. Using an electronic platform scale, each block can be weighed and either accepted or rejected on delivery. In accordance with the specification, each block was required to have weight, production date and resin source labels. Production quality control records are also

maintained by manufacturers. Such data can be required to be made available in the purchase agreement. The blocks were specified and delivered in 2.4m (8ft) lengths. Manufacturers commonly produce blocks in 4.8m (16ft) lengths. Wherever possible, blocks should be installed in 4.8m (16ft) lengths to reduce the frequency of vertical gaps. Blocks should be installed with staggered joints to prevent continuous vertical joints between successive layers everywhere.

Situations for rapid construction arise from re-building after a disaster or in planned replacement of substandard infrastructures along existing highways (16). Geofoam producers mostly operate one block molding unit per plant. Daily production capacity is limited and the process of pre-expansion, aging, molding and curing require lead time. Manufacturers may not have sufficient rolling stock in both resin supply and EPS blocks to meet the large volume supply required for rapid construction while meeting normal demand from regular customers. Even following proper analysis, design, quality assurance and installation practice, production limitations may cause delays, poorly formed blocks and pre-mature delivery of blocks to the site. Partitioning the order to multiple suppliers to increase capacity has limitations in that manufacturers do not produce blocks of the same height. The challenges of quality assurance and supply of good quality blocks within a short time window can be managed better by maintaining a reasonable supply of pre-produced blocks. A supply of good quality blocks can be available right away without rush production and quality assurance effort in the aftermath of a disaster. Segmental pre-cast concrete slabs can also be stockpiled for use as readymade load distribution slabs. Both stockpiled geofoam blocks and pre-cast concrete slabs can be used as running stock for regular projects. Based on experience gained from previous applications and lessons learned from the

I88 failure, setting a new state of practice for rapid construction with geofoam can save time and improve the project delivery process.

Suggestions

With aging culverts, more frequent intense storms with global warming and sea level rise (17); there will be increasing need for rapid reconstruction in the tri-state region of NJ, NY and Connecticut, as well as elsewhere. Based on the findings of this investigation and prior successful applications, the following suggestions are provided to improve the state of rapid construction practice using geofoam:

- Limit vertical pressures from dead and live loads to less than 50% of the unconfined compression strength at 10% strain or stress at 1% strain, whichever is less.

- Avoid continuous vertical joints between successive geofoam layers.

- Provide a stepped transition between soil and geofoam interfaces placing geofoam blocks on top and not below compacted soil.

- Request the manufacturer to provide in plant quality control data for all supplied blocks and also weigh blocks to accept or reject on delivery or implement a robust quality assurance program.

- Require full size blocks to meet the specified density as a minimum and not exceed the specified density by more than 10%.

- Specify full lengths (16ft) rather than half lengths (8ft) blocks unless necessary to form specific shapes or edges.

- Provide base and side internal drainage and direct surface flow away from the geofoam fill area to prevent submersion of blocks and high groundwater levels.

- Use a load distribution slab over geofoam surfaces below road lanes or consider installing geogrids to attenuate stress increments from compaction during construction.

- Consider stockpiling geofoam blocks and pre-cast load distribution slab segments as rolling stock for regular projects and for emergency construction.

Acknowledgements

NYSDOT facilitated the investigation and provided valuable assistance. Shelter Enterprises Inc., provided test samples and financial support. Funding for the study was provided by US DOT Region 2 University Transportation Research Center (UTRC).

References

1. NYSDOT, 2006 - 2007 Emergency Structure Replacement Report, Interstate 88 over Carrs Creek, Albany, NY, 2009.
2. SRBC, Susquehanna River Basin Commission, June 2006 Flood, Harrisburg, PA, 2007.
3. NYS Highway Bridge Data: https://www.dot.ny.gov/main/bridgedata
4. Negussey, D. and Jahanandish, M., A Comparison of Some Engineering Properties of EPS to Soils. Transportation Research Record, No. 1418, 1993.
5. Sheeley, M., Slope Stabilization Utilizing Geofoam, MSc Thesis, Syracuse University, Syracuse, NY, 2000.
6. Srirajan, S., Recycled Content and Creep Performance of EPS Geofoam in Slope Stabilization, MSc Thesis, Syracuse University, NY, 2001.

7. FLAC V.6., Fast Lagrangian Analysis of Continua-V.6.0.387. Itasca Consulting Group, Inc., Minneapolis, MN, 2008.
8. Singh, S. T. MSc Thesis, (upcoming), 2014.
9. Birhan, A. G. Effect of Confinement and Temperature on the Behavior of EPS Geofoam. PhD Thesis, Syracuse University, Syracuse, NY, 2014.
10. Sun, M. C. Engineering behavior of expanded polystyrene geofoam and lateral pressure reduction in substructures. MSc Thesis, Syracuse University, Syracuse, NY, 1997.
11. Anasthas, N., Negussey, D., and Srirajan, S. Effect of confining stress on compressive strength of EPS geofoam. Proceedings of 3rd International Conference of EPS Geofoam, Salt Lake City, UT, 2001.
12. Birhan, A., and Negussey, D. Effects of confinement on the stress strain behavior of EPS geofoam. International Conference on Geotechnical Engineering, Shanghai, China, 2014.
13. Birhan, A., and Negussey, D. Effect of Confinement on Creep Behavior of EPS Geofoam, ASTM Geotechnical Journal, 2014 (accepted for publication)
14. Negussey, D., and Stuedlein, A. W. Geofoam fill performance monitoring. Utah Department of Transportation, Rep. No. UT, 3, Salt Lake City, UT, 2003.
15. Elragi, A., Negussey, D., and Kyanka, G. Sample size effects on the behavior of EPS geofoam. Soft Ground Technology, ASCE Geotechnical Special Publication, 2001.
16. Performance Specifications for Rapid Highway Renewal, Strategic Highway Research Program, SHRP-2, Report S2-R07-RR-1, Transportation Research Board, Washington, DC, 2014.
17. Vulnerability of Transportation System and Evacuation Plan for Coastal Flooding in Climate Change, University Transportation Research Center - Region 2, Final Report, 2014.

Figures

FIGURE 1 Location of the Carrs Creek culvert failure (Google Maps).

FIGURE 2 The Carrs Creek culvert on I88 collapsed (1). Carrs Creek quickly eroded the road embankment and culvert side fill to form a wide gulley.

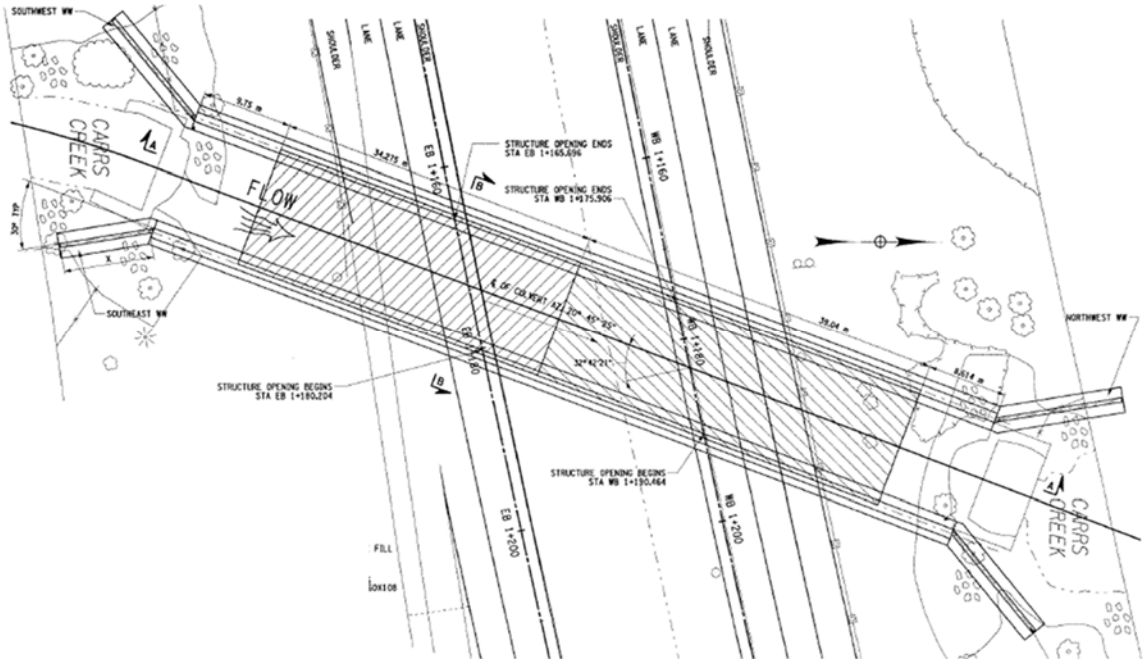

FIGURE 3 The Carrs Creek culvert re-construction in plan.

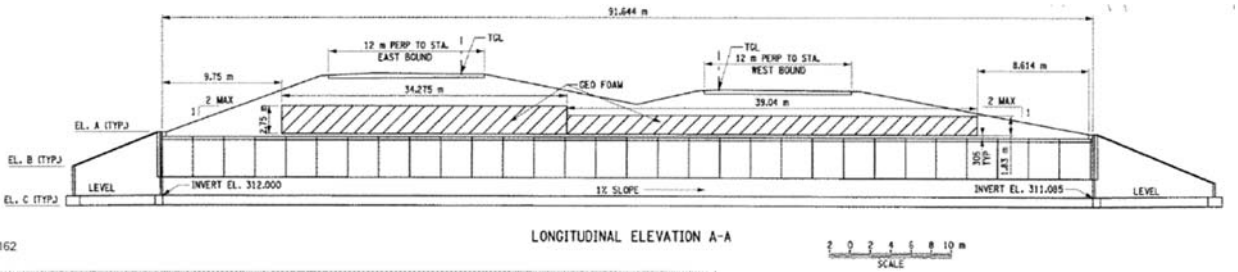

FIGURE 4 The Carrs Creek re-construction in longitudinal elevation (1).

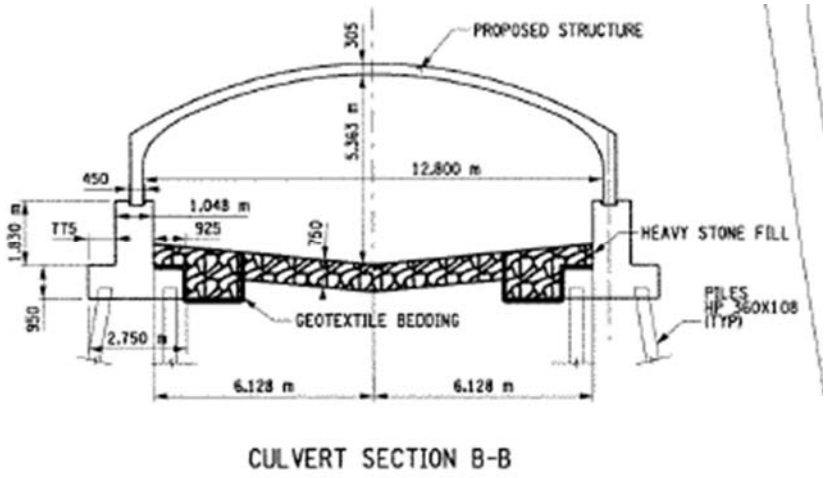

FIGURE 5 The Carrs Creek re-construction in transverse section (1).

FIGURE 6 Three sided pre-cast concrete segments and foundation.

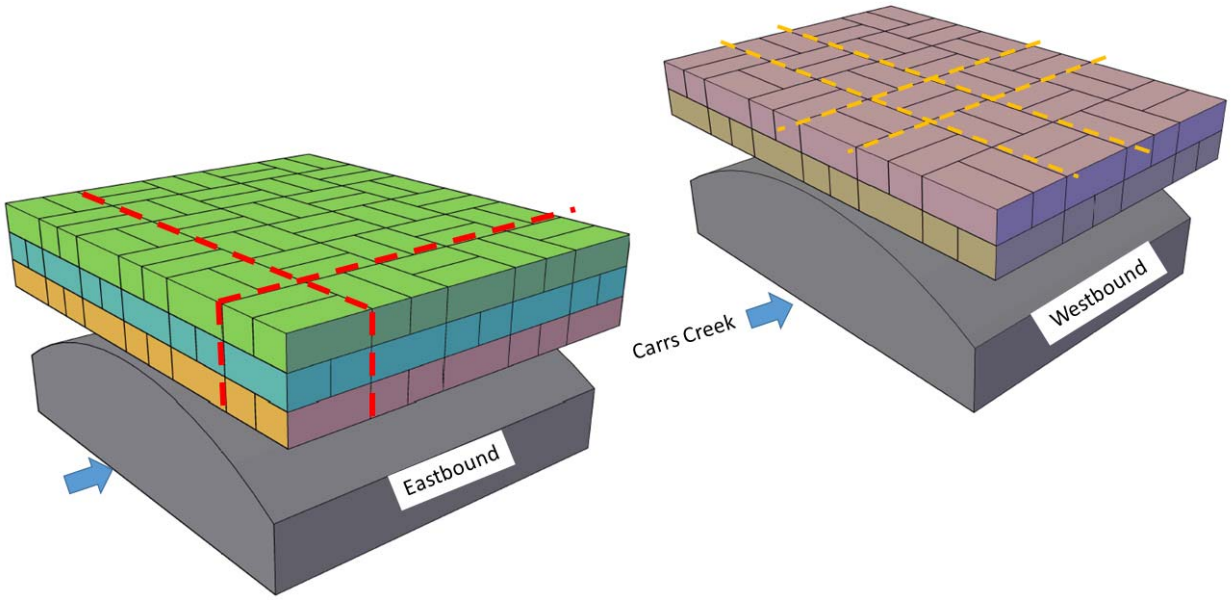

FIGURE 7 Geofoam block orientations were rotated in successive layers but the installation featured continuous vertical joints at 2.4m (8ft) spacing.

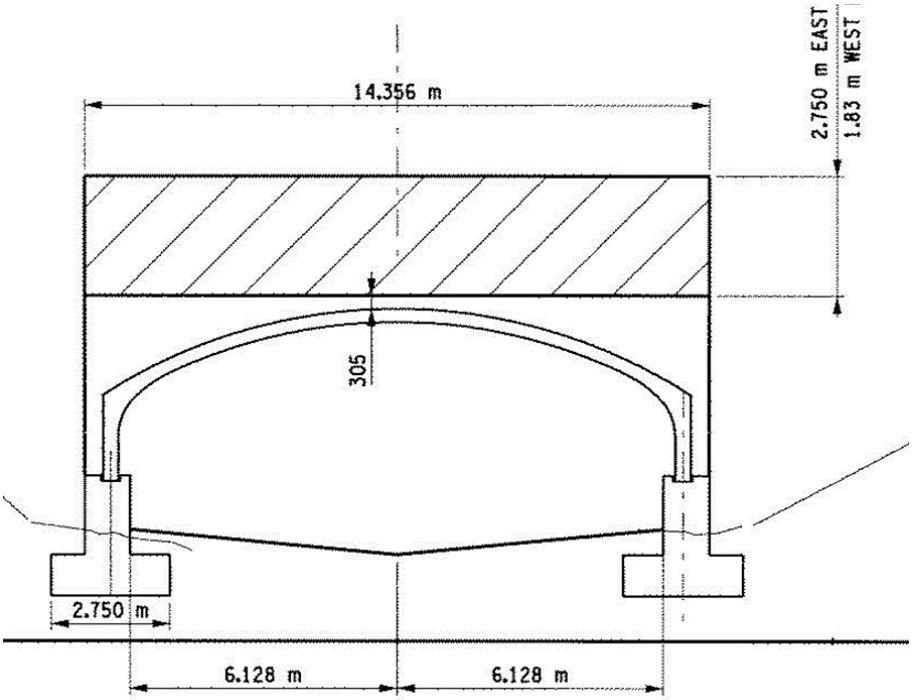

FIGURE 8 Pre-cast concrete culvert section and the geofoam fill position. The bedding thickness below the geofoam is 0.3m (1ft) at center and about 1.8m (6ft) above the side walls (1).

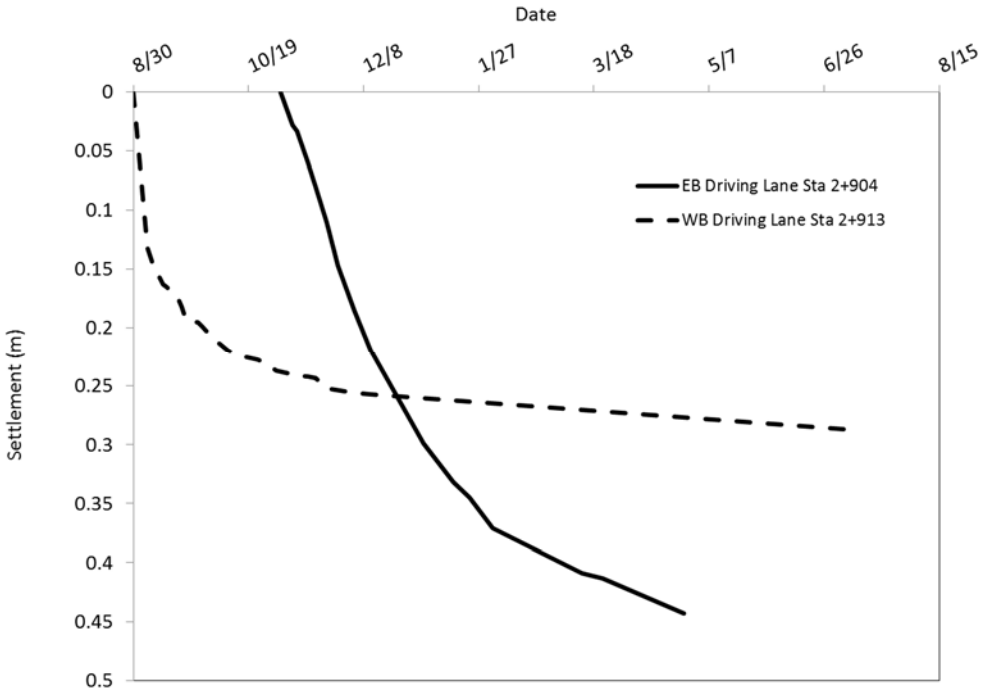

FIGURE 9 Cumulative settlements at eastbound 2+904 and westbound 2+913. Paving of the eastbound was delayed after placement of the compacted soil.

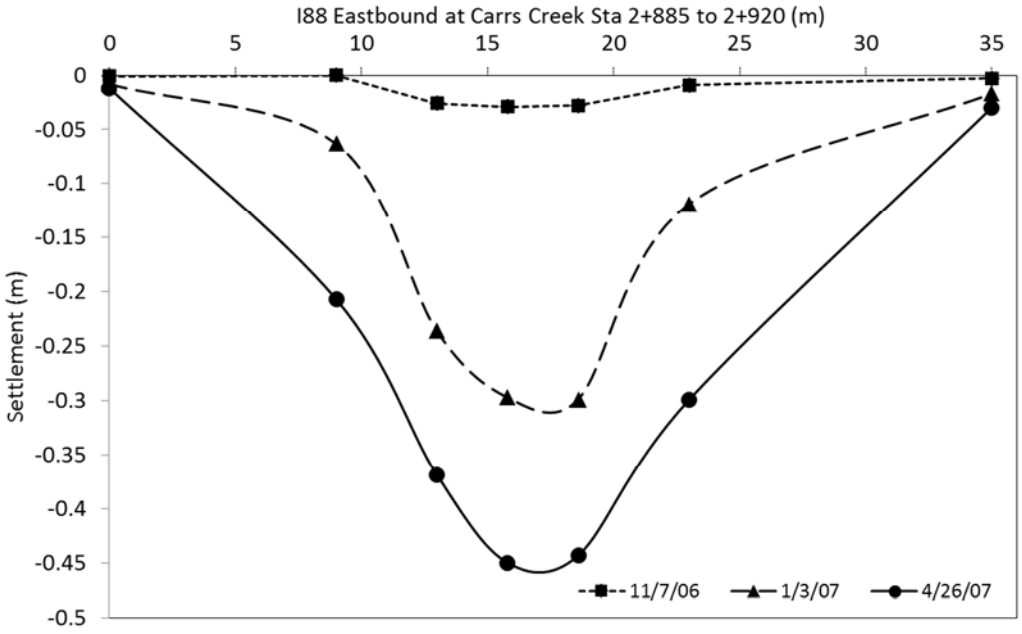

FIGURE 10 Settlements across eastbound from 2+885 to 2+920 (1). The magnitude of settlements was lower than actually occurred as observations started after delayed paving.

FIGURE 11 Exhumed blocks from eastbound south side slope. Blocks towards the forefront are not as heavily loaded and deformed.

FIGURE 12 Exhumed geofoam from below eastbound I88 roadway. See the unequal deformations of four adjacent blocks behind the shovel at left of center.

FIGURE 13 Perched water on the geomembrane cover above the geofoam.

FIGURE 14 Perched water between the culvert top and the geofoam base (1).

FIGURE 15 Removing the geomembrane cover from the geofoam at the south end of the culvert below the eastbound embankment (1).

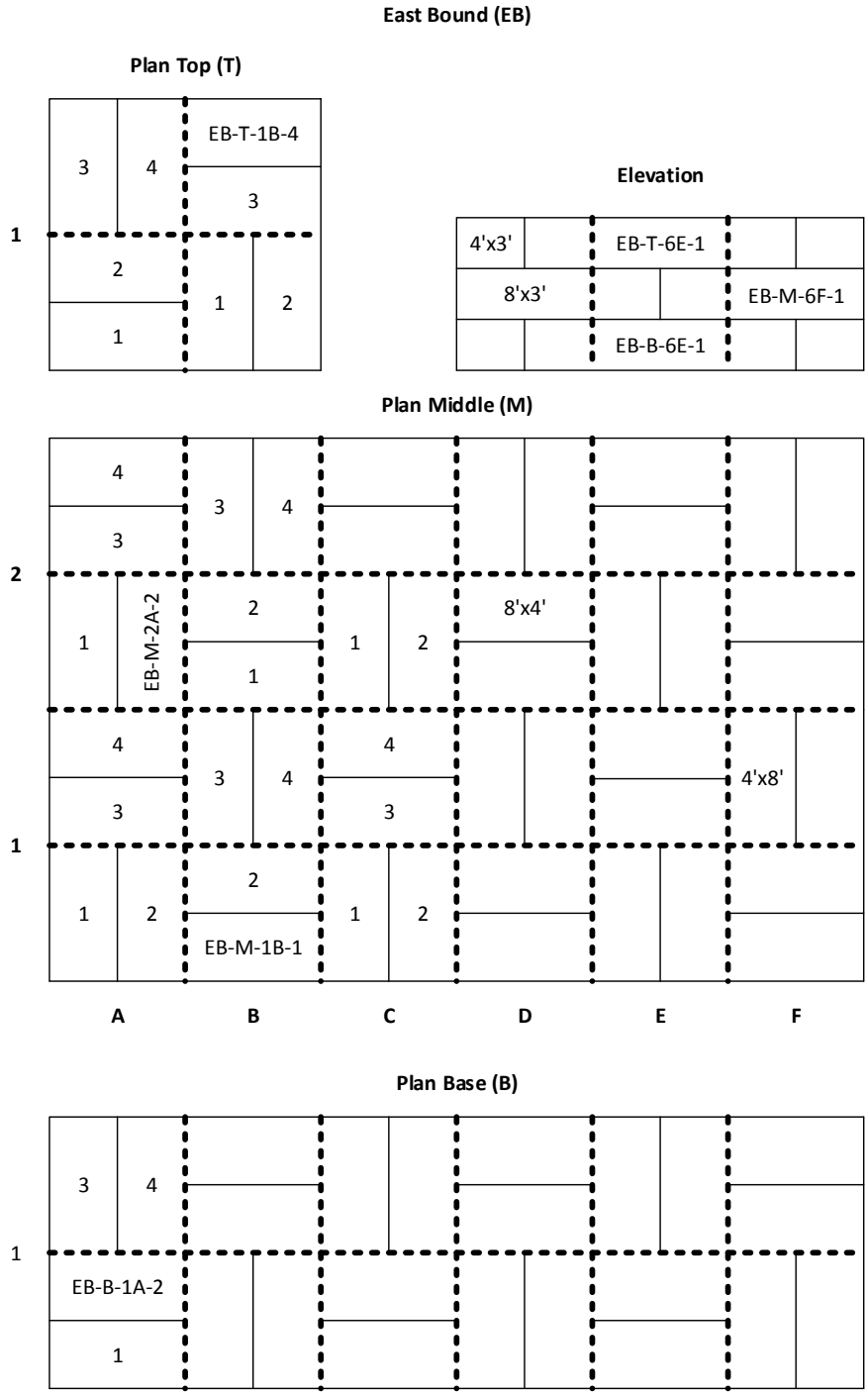

FIGURE 16 Block naming convention developed by cross referencing the exhumed data set with the block layout plans for the re-construction (1). (EB or WB, travel direction) – (B, M, T; base, middle, top; layer) – (4.8m (16ft) wide numbered transverse rows from 1 to 15) – (2.4m (8ft) wide lettered longitudinal rows from A to F). The top and base layer patterns matched.

FIGURE 17 Stockpile of exhumed blocks from 2006. (Google Maps 2014).

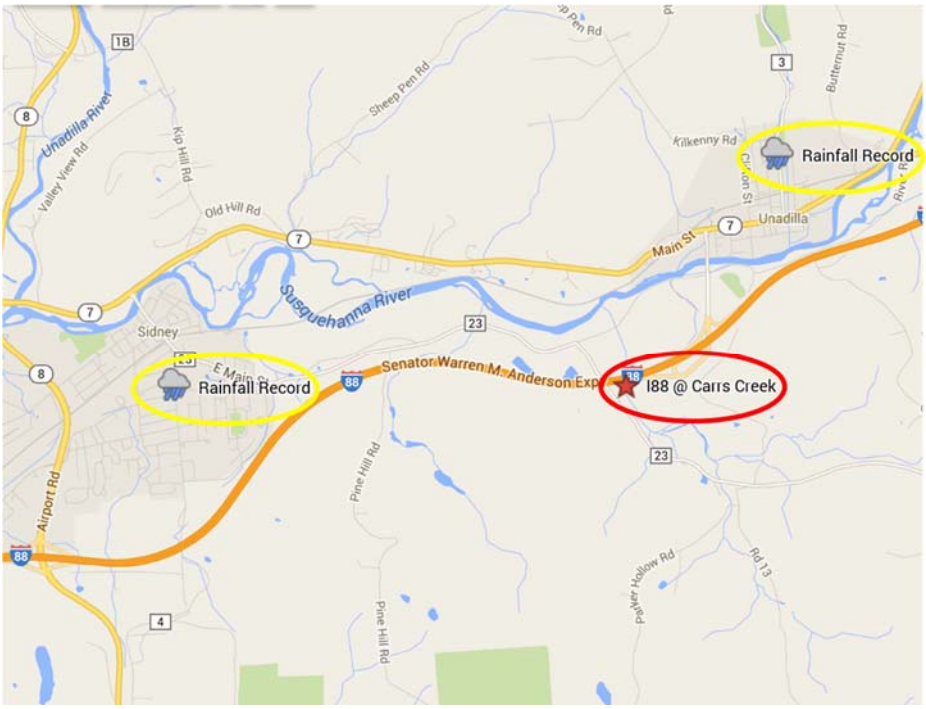

FIGURE 18 Carrs Creek location between Sidney and Unadilla, NY (Google Maps). The highest ever flood elevation of the Susquehanna River at Unadilla was on June 28, 2006.

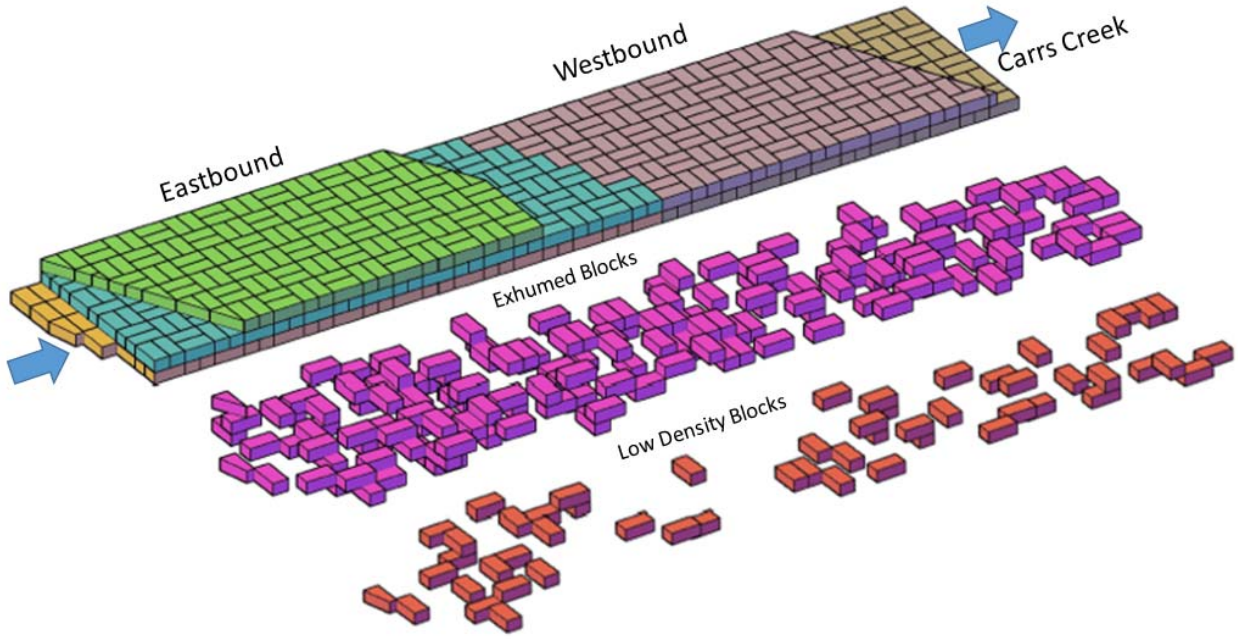

FIGURE 19 Three D model of geofoam layers, exhumed blocks and low density blocks.

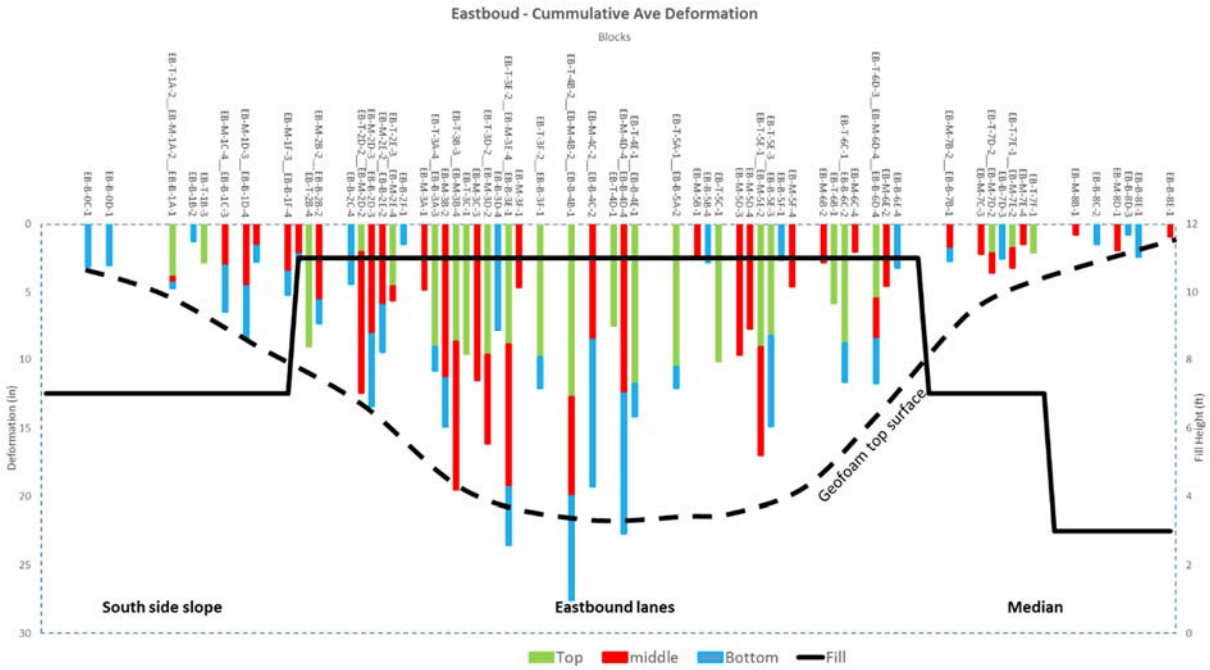

FIGURE 20 Cumulative average deformations and approximate geofoam top surface profile of I88 eastbound from measurement of exhumed blocks.

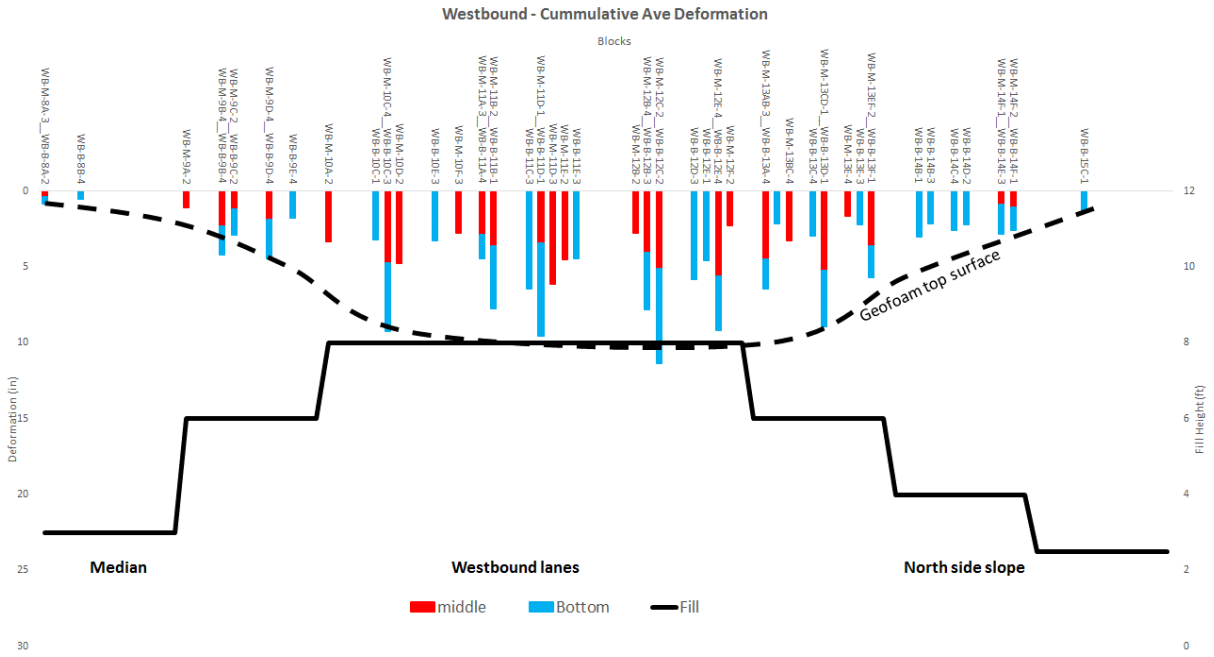

FIGURE 21 Cumulative average deformations and approximate geofoam top surface profile of I88 westbound from measurement of exhumed blocks.

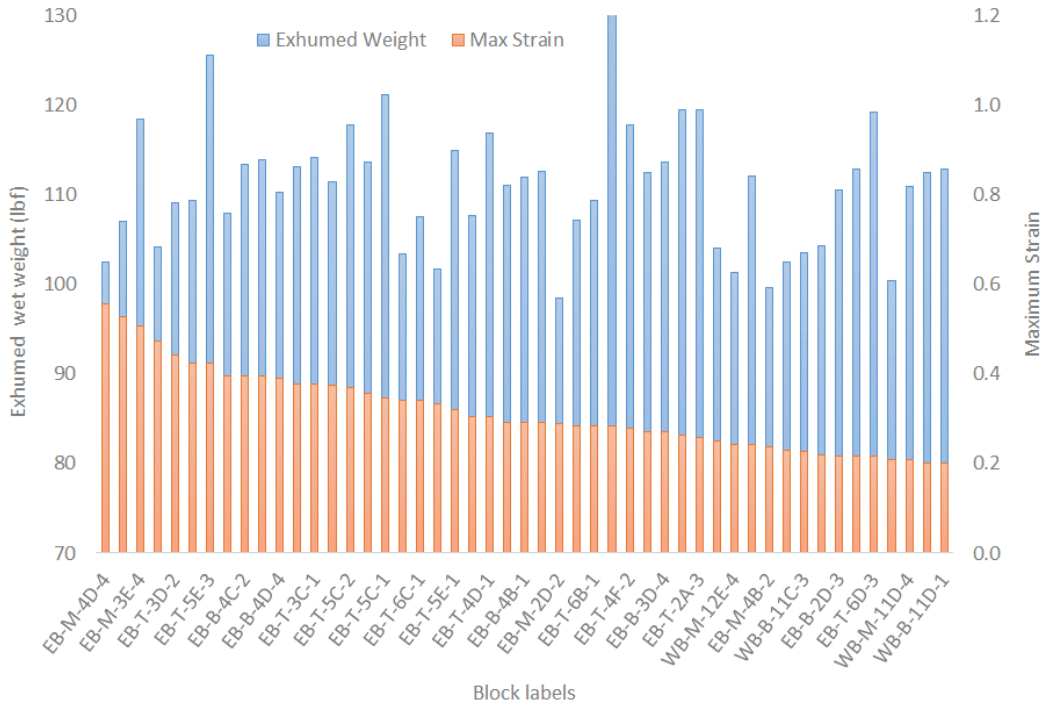

FIGURE 22 Maximum vertical strain and weight of exhumed geofoam blocks. From a ranked list of 25 blocks with highest vertical strain, the top 17 were from below the eastbound.

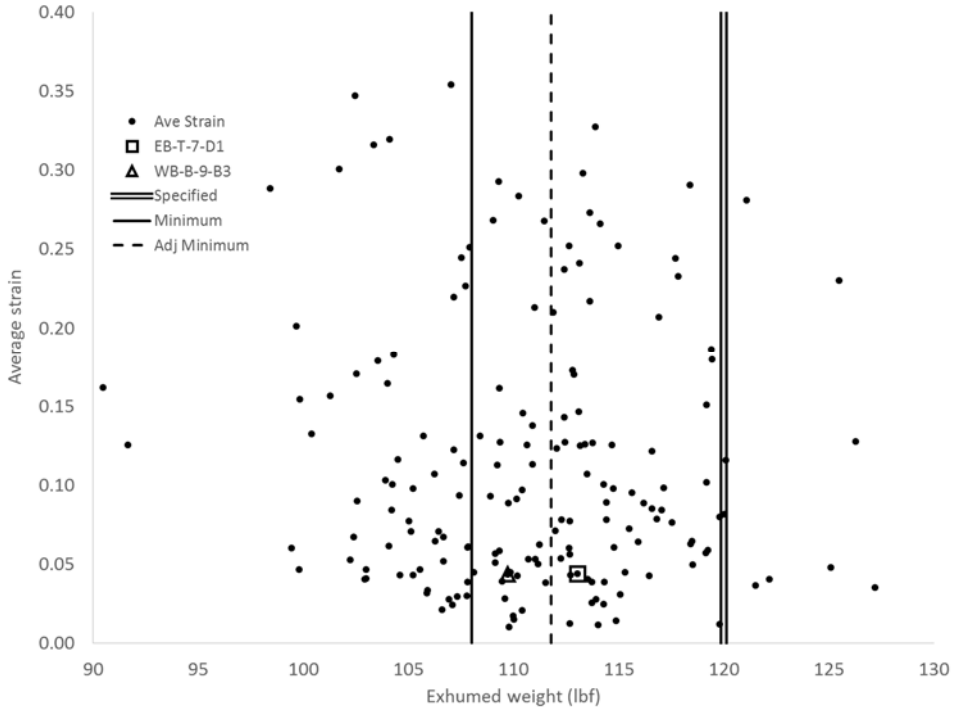

FIGURE 23 Average strain and exhumed weights of geofoam blocks. The nominal weight for the specified density blocks was 0.54kN (120lbf). At 10% tolerance, the minimum acceptable weight was 0.49kN (108lbf). Based on adjusted minimum for wet weights of 0.51kN (111.8lbf) almost half of the exhumed blocks were unacceptable.

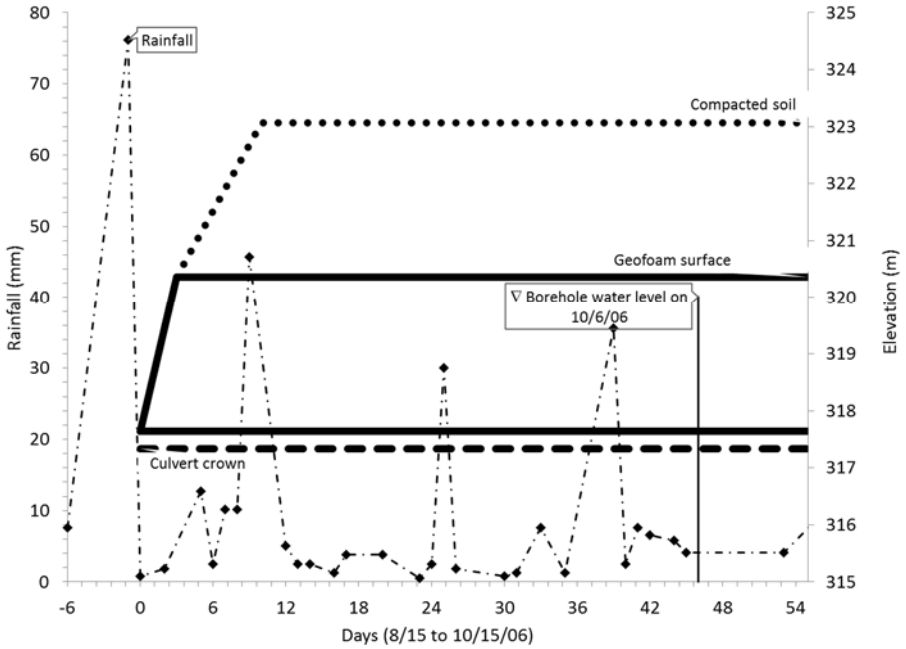

FIGURE 24 Precipitation record for Carrs Creek at I88 during and post construction.

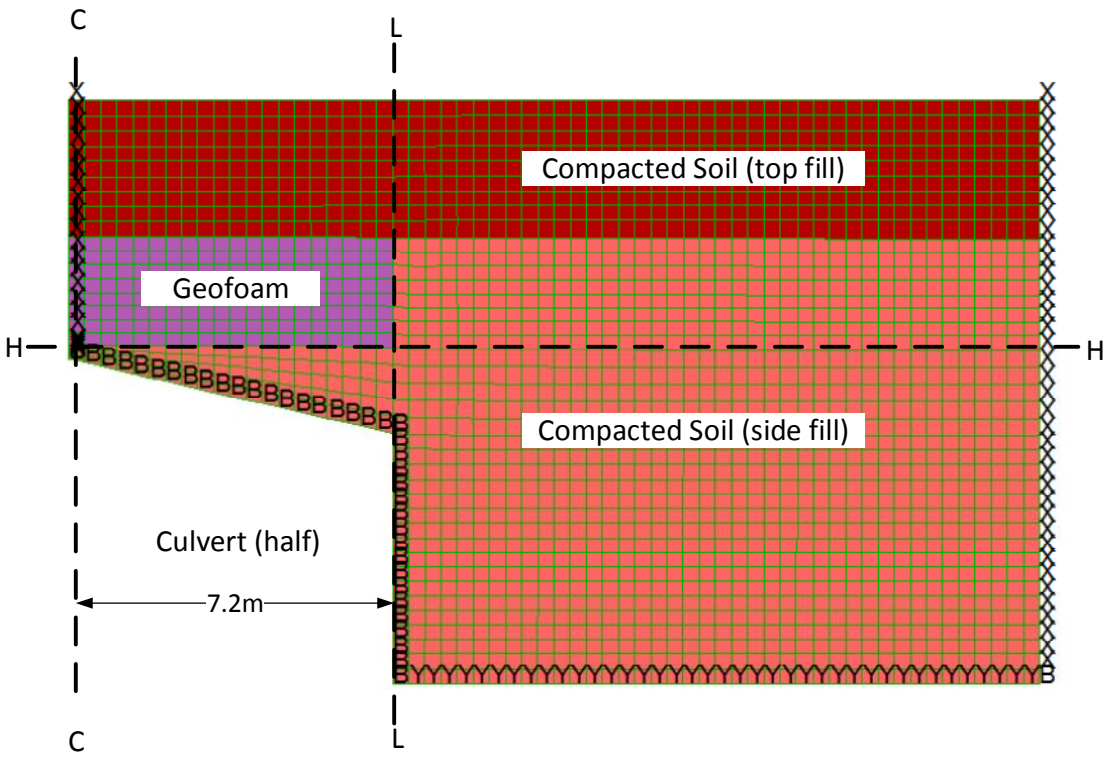

FIGURE 25 A FLAC model of the geofoam, culvert and compacted soil as built in profile for eastbound lanes. Due to symmetry about the center axis, the model is only half of the section.

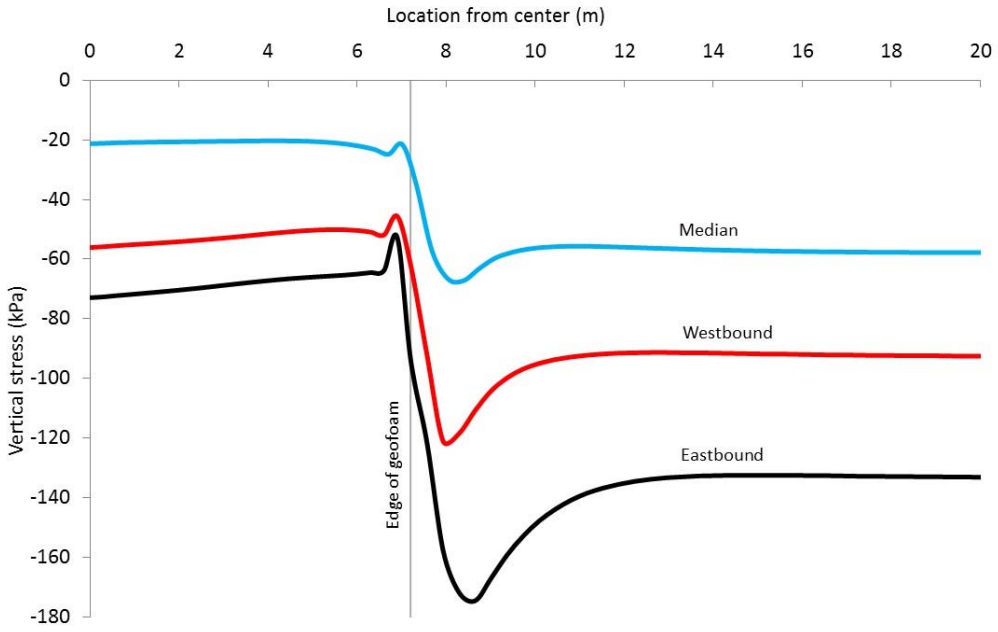

FIGURE 26 Vertical pressure profiles from FLAC modeling for the eastbound, median and westbound as built sections.

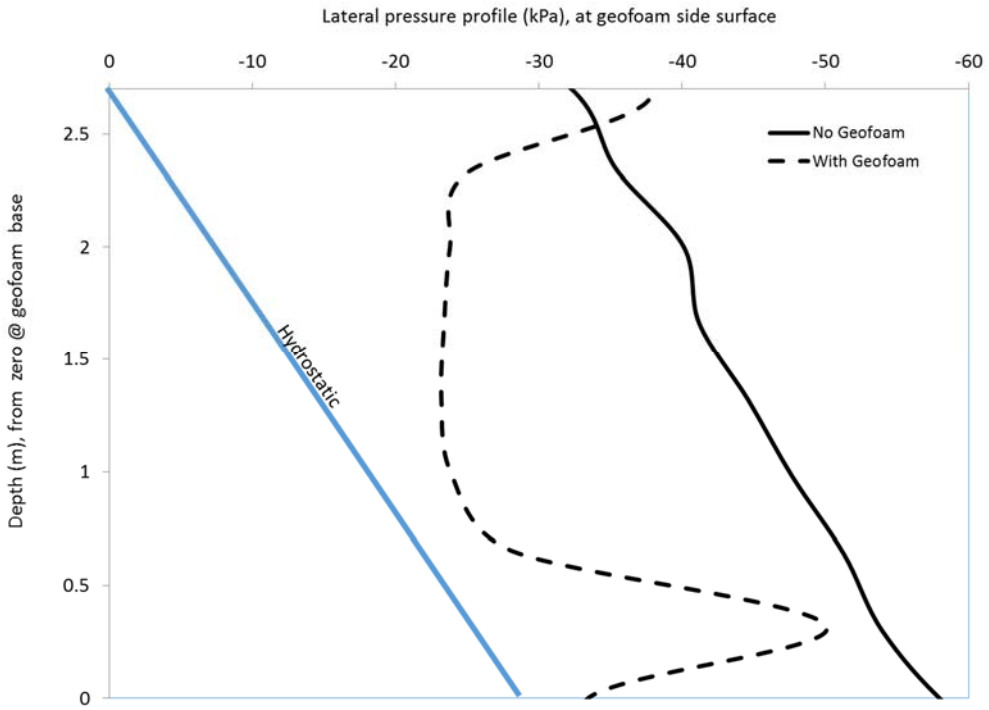

FIGURE 27 Horizontal soil pressure from FLAC models, at the soil/geofoam interface position for cases with and without geofoam of the eastbound as built profile. Also shown is additional hydrostatic pressure for water level at the geofoam surface when the median becomes flooded.

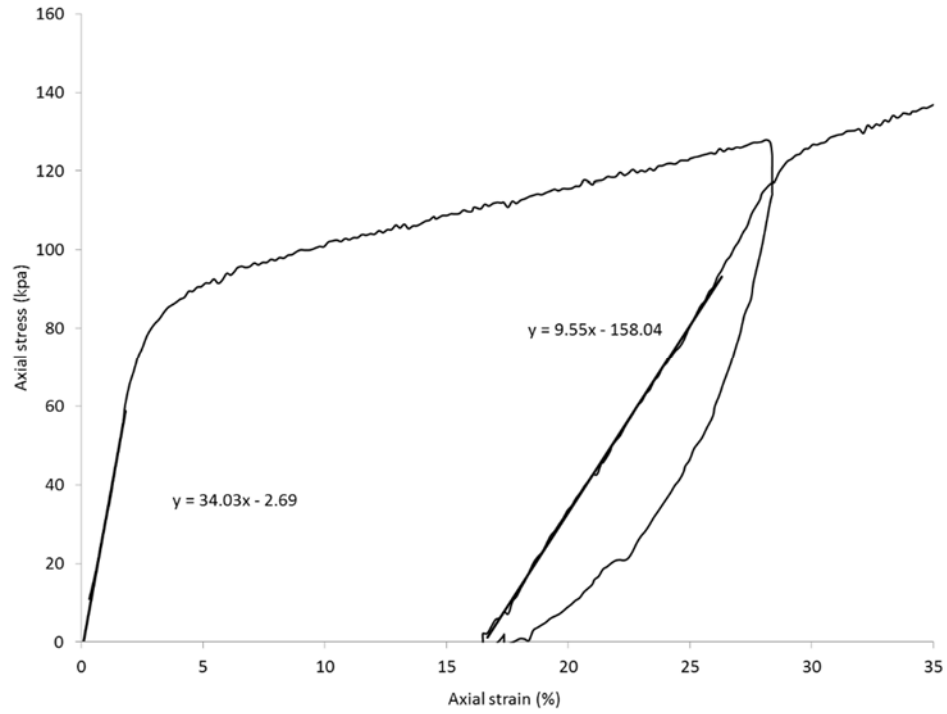

FIGURE 28 Pre-strain and modulus degradation of geofoam in unconfined compression.

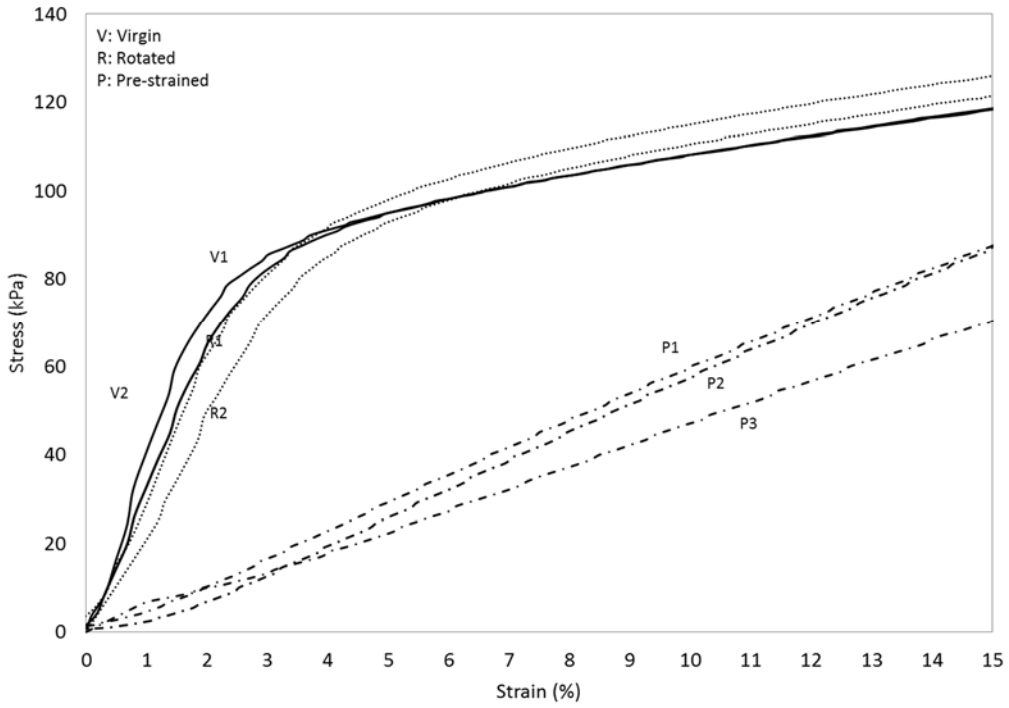

FIGURE 29 Pre-strain effect and modulus degradation of exhumed blocks.

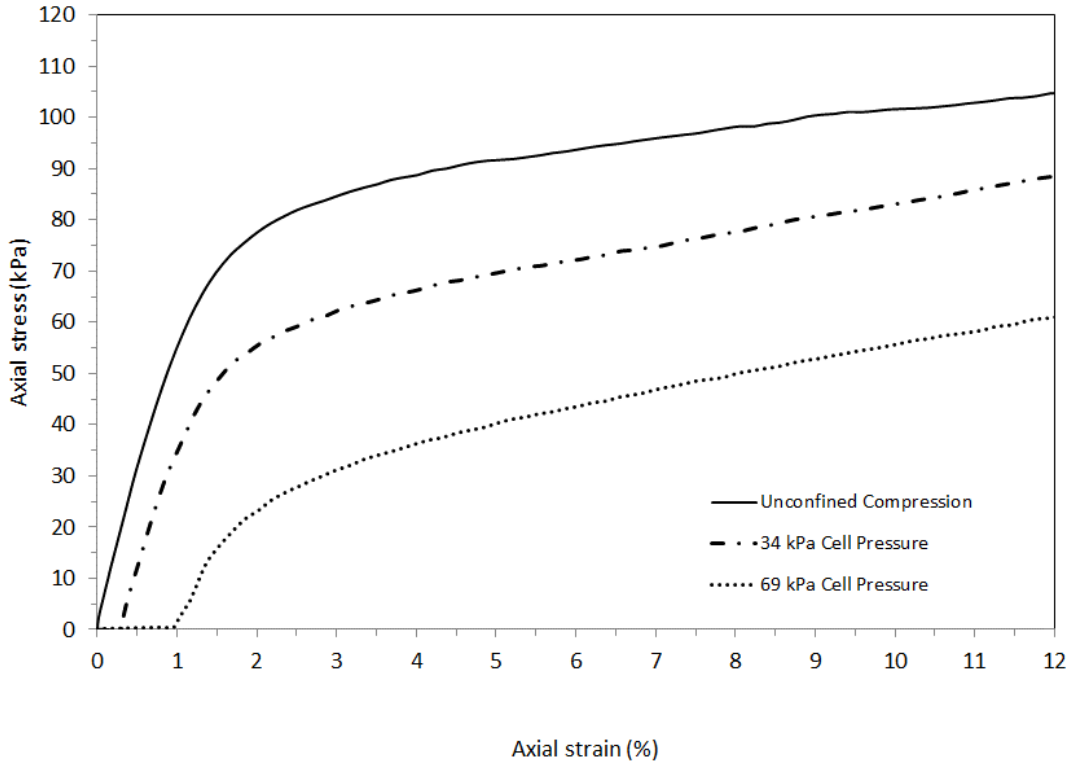

FIGURE 30 Effect of confining pressure on geofoam response to uniaxial loading.

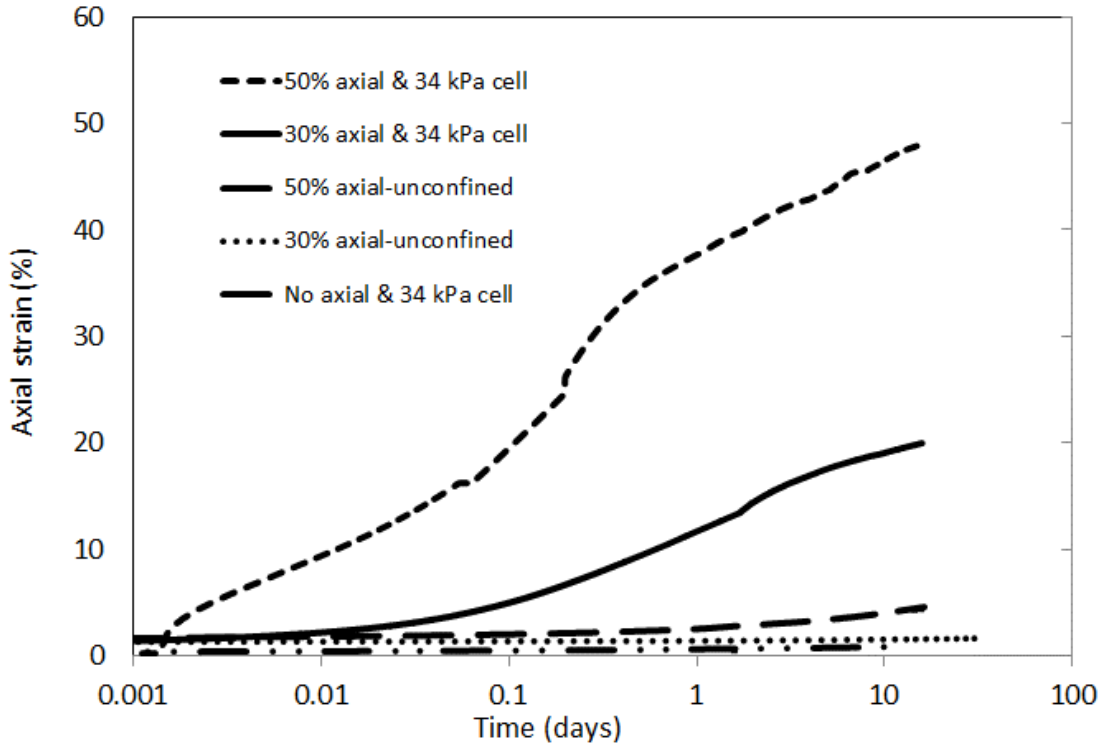

FIGURE 31 Effect of confining pressure on development of creep strains.

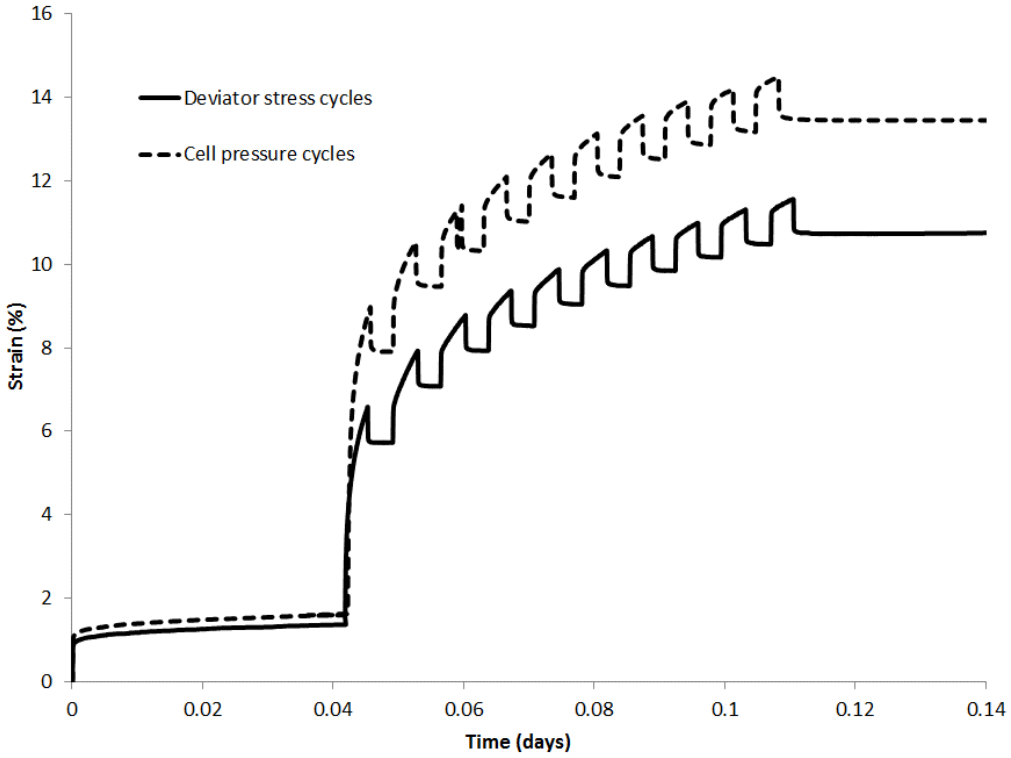

FIGURE 32 Strain accumulation in response to cyclic load increments in undrained loading.

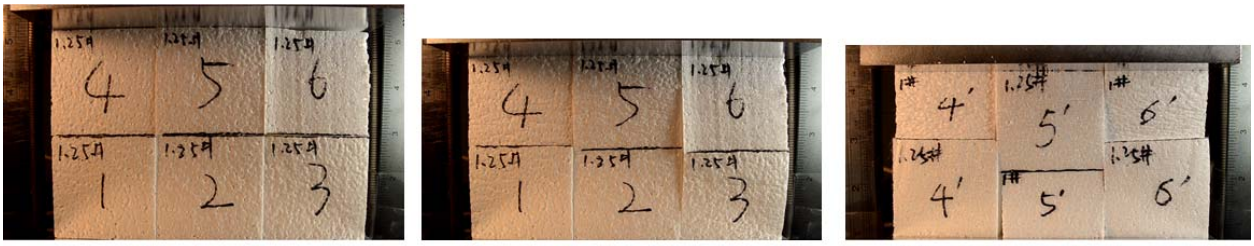

FIGURE 33 Compression of uniform and mixed density block layers with continuous gaps.

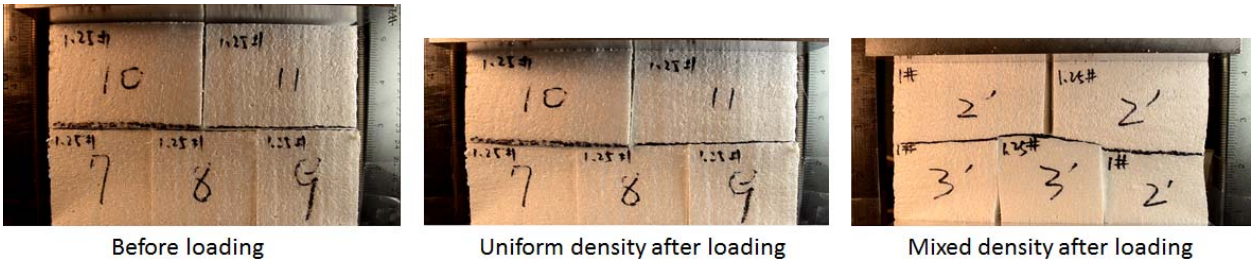

FIGURE 34 Compression of uniform and mixed density block layers with staggered gaps.

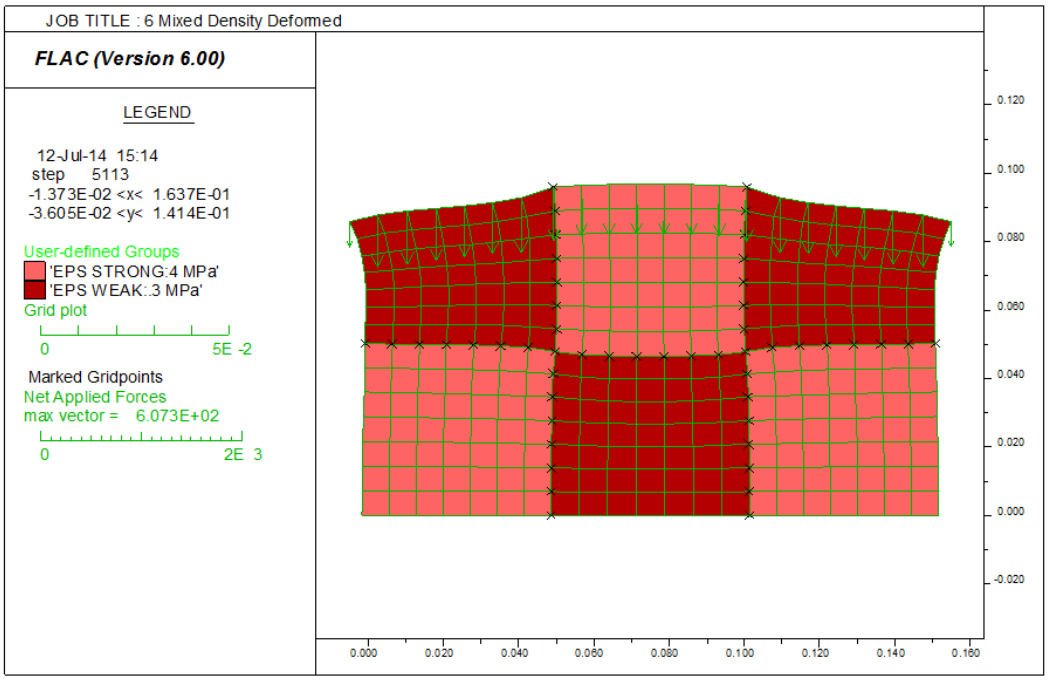

FIGURE 35 FLAC model deformations of constant pressure loading of mixed density geofoam layers with continuous vertical gaps. Low density blocks deformed more than high density.

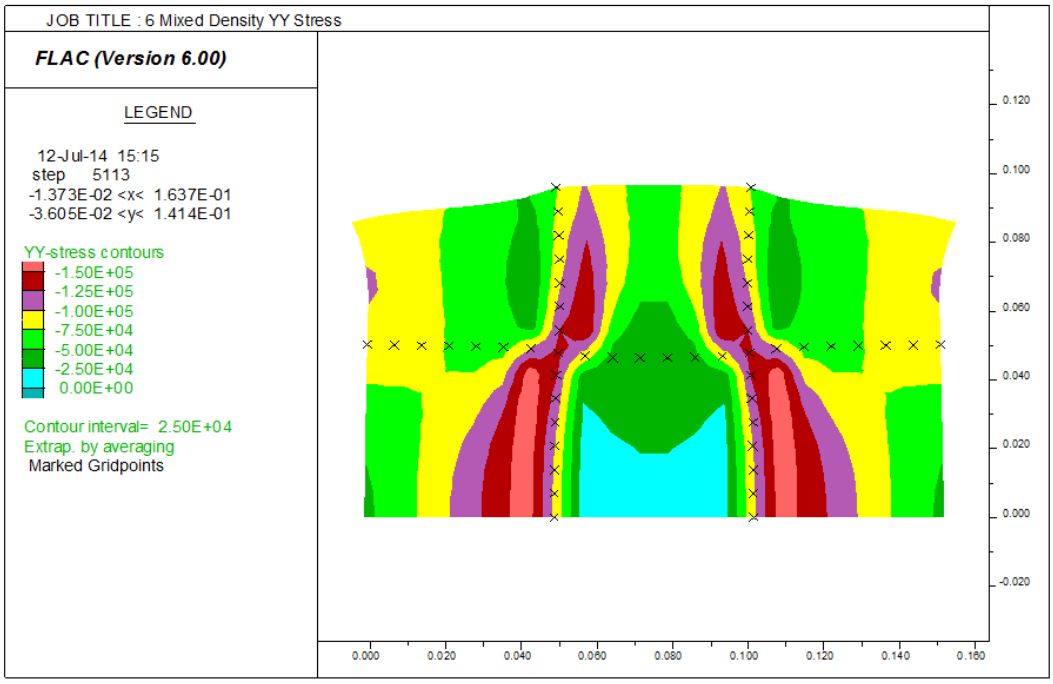

FIGURE 36 FLAC model stresses of constant pressure loading of mixed density geofoam block layers with continuous vertical gaps. Stresses much higher than the applied constant boundary pressure developed in the higher density blocks adjacent to lower density blocks.

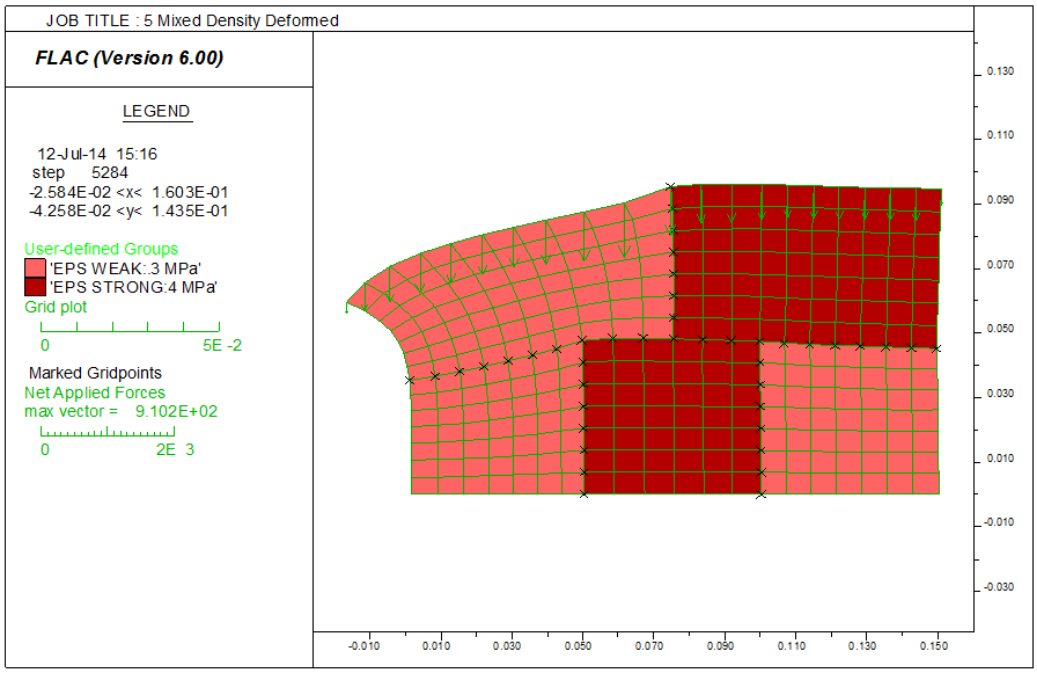

FIGURE 37 FLAC model deformations of constant pressure loading of mixed density geofoam block layers with staggered vertical gaps. The lower density blocks deformed more than the higher density blocks.

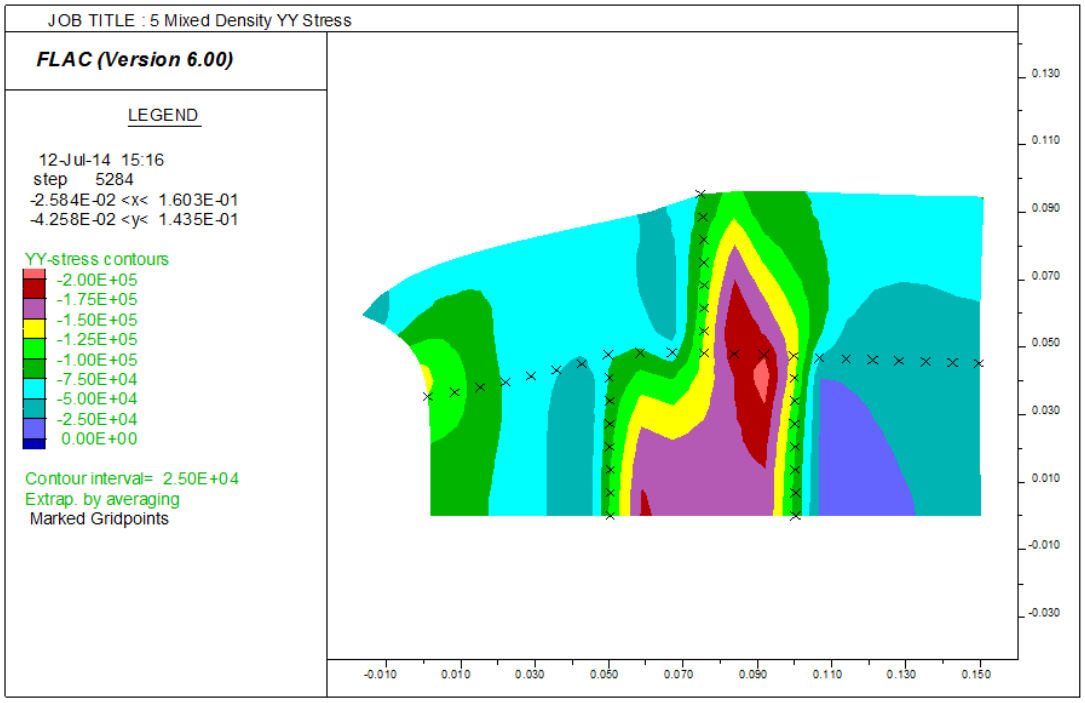

FIGURE 38 FLAC model stresses of constant pressure loading of mixed density geofoam block layers with staggered vertical gaps. Stresses much higher than the applied constant boundary pressure develop in the connected higher density blocks.

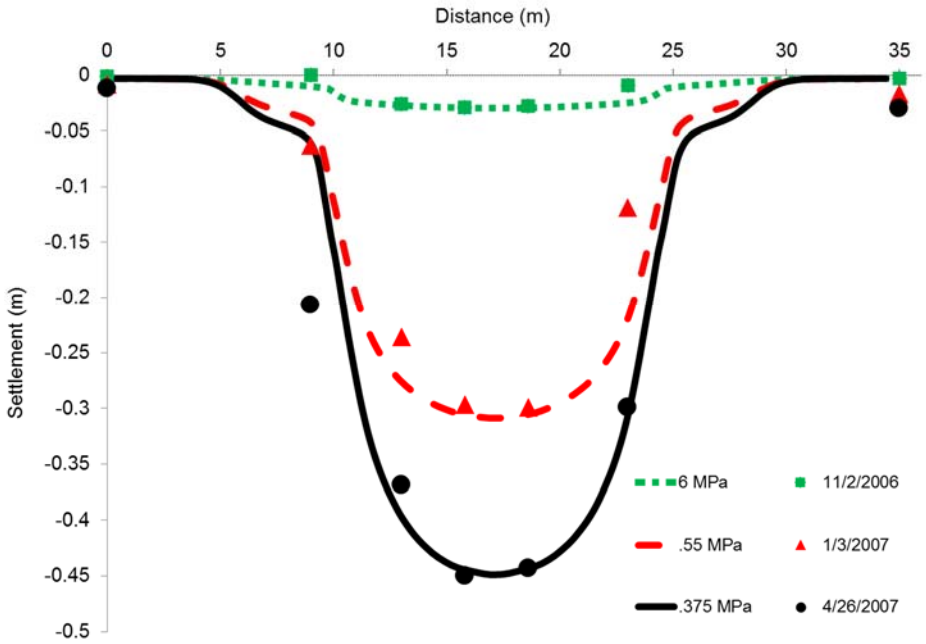

FIGURE 39 Model simulations of observed settlements; eastbound from 2+885 to 2+920 (1).

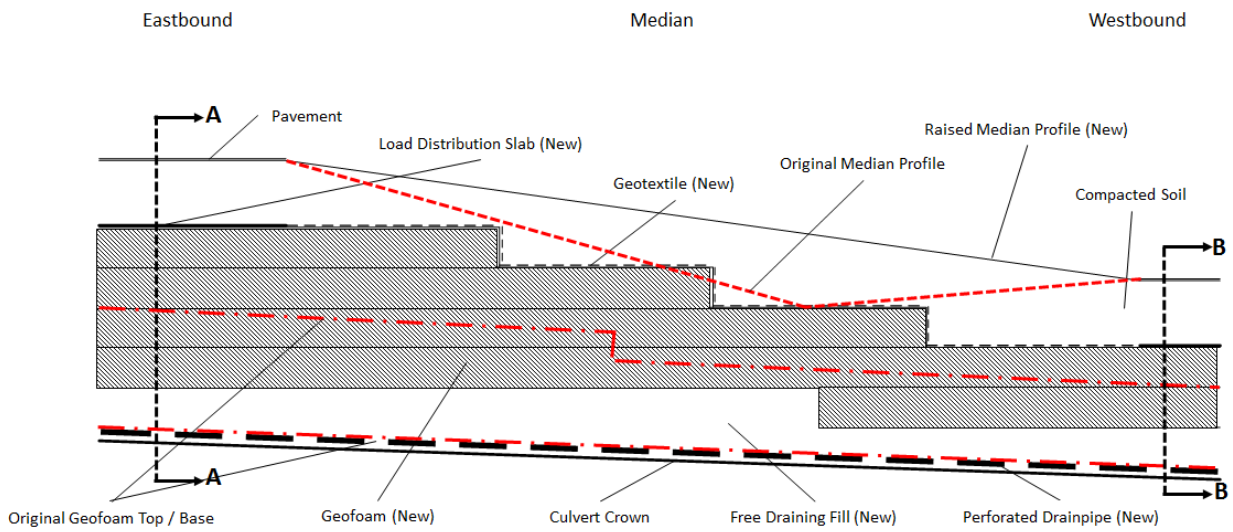

FIGURE 40 As built (original) and alternate (new) design profiles at the culvert centerline.

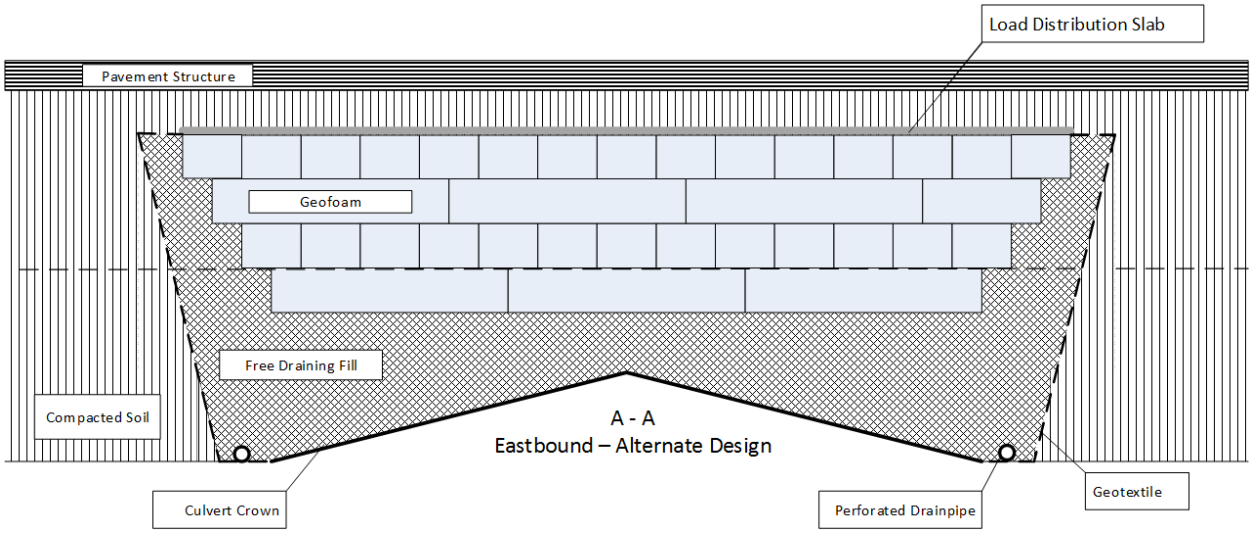

FIGURE 41 The proposed alternate design profile for I88 eastbound.

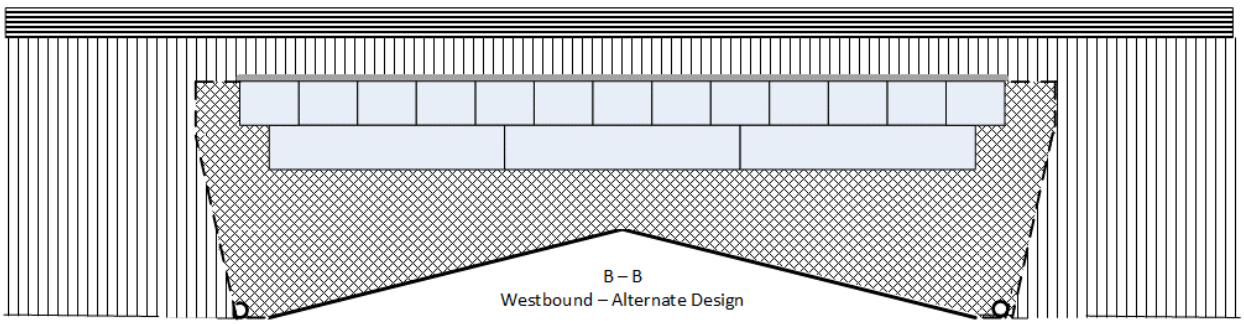

FIGURE 42 The proposed alternate design profile for I88 westbound.

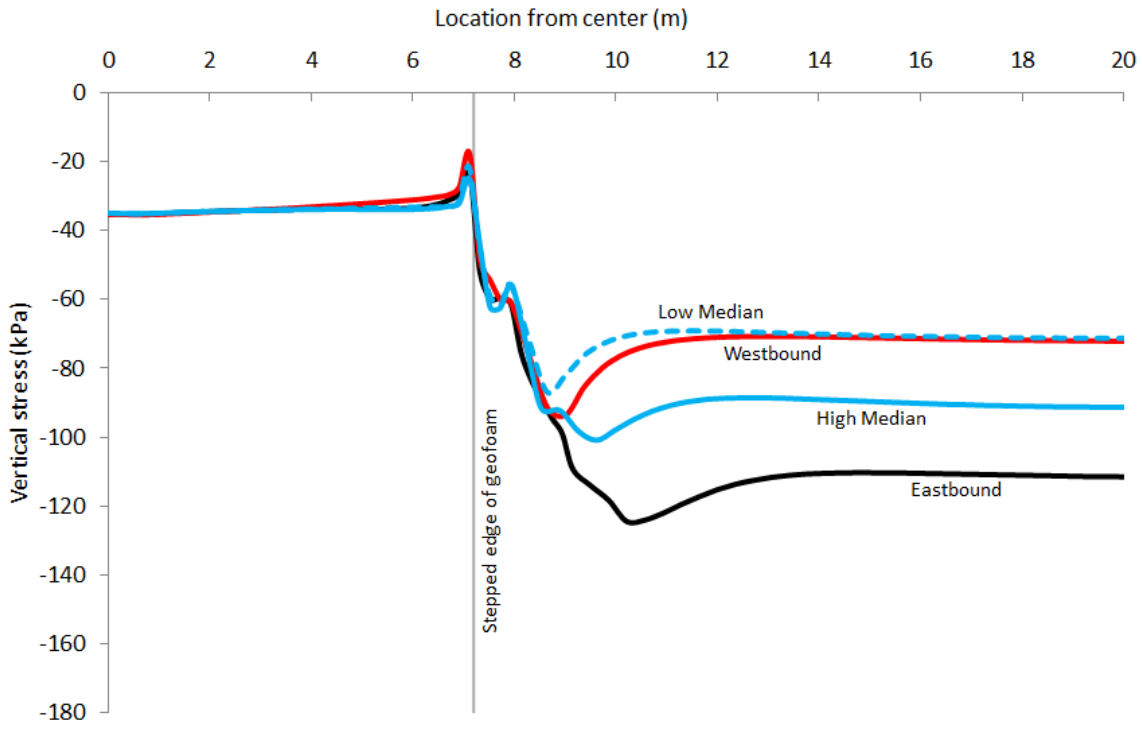

FIGURE 43 Vertical pressure profiles from FLAC modeling for the eastbound, median and westbound of proposed (new) sections.

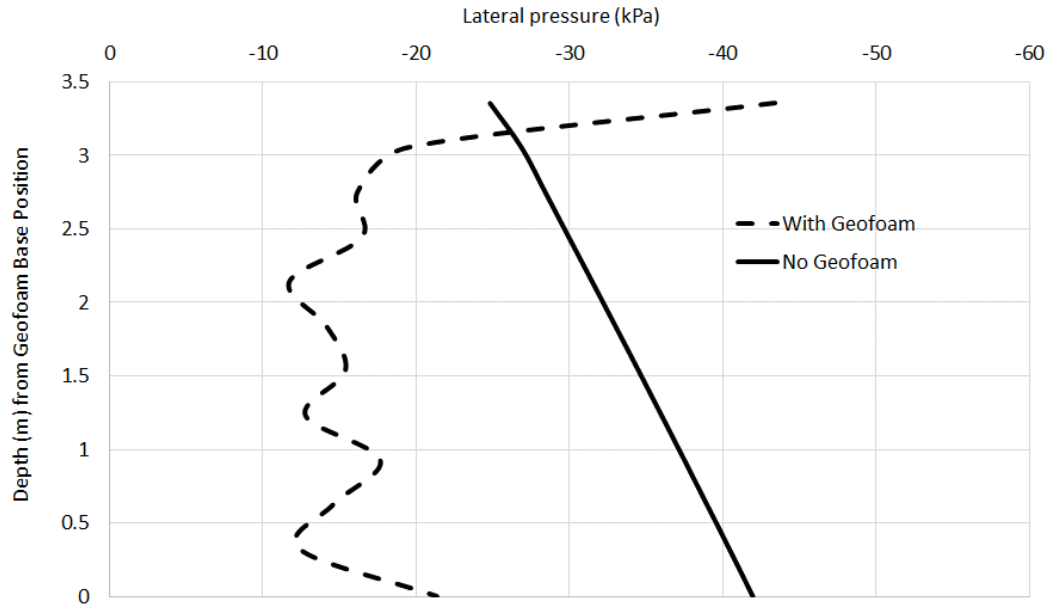

FIGURE 44 Lateral pressure profiles from FLAC modeling for the revised eastbound at geofoam edge position, with and without geofoam; compare with the as built section in Figure 27. No hydrostatic pressure because drainage is provided.

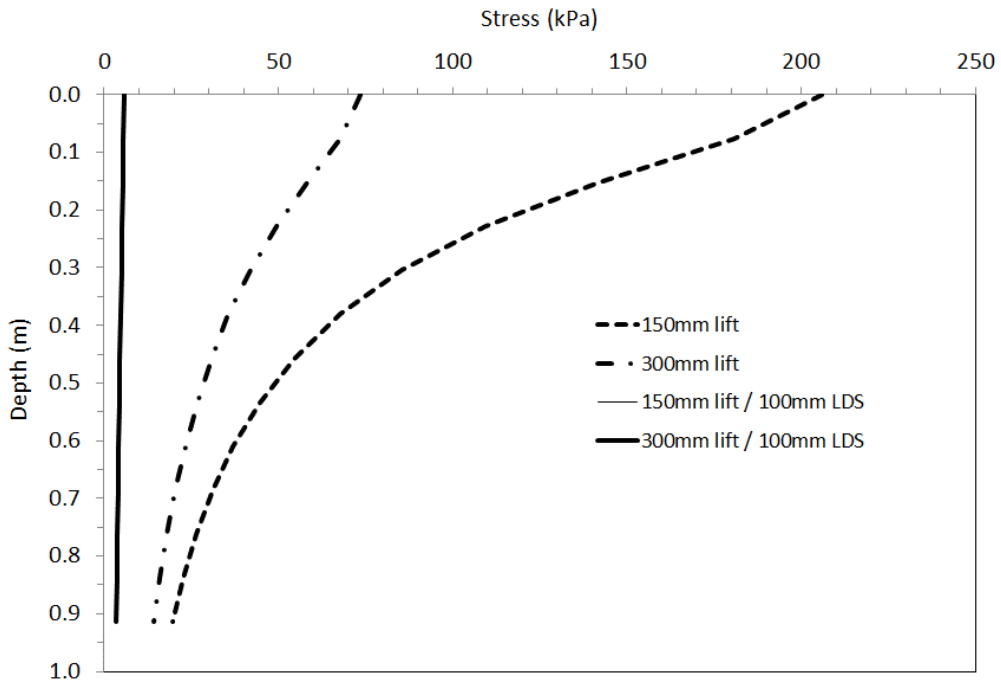

FIGURE 45 Compaction induced stresses in geofoam blocks w/without concrete slabs.

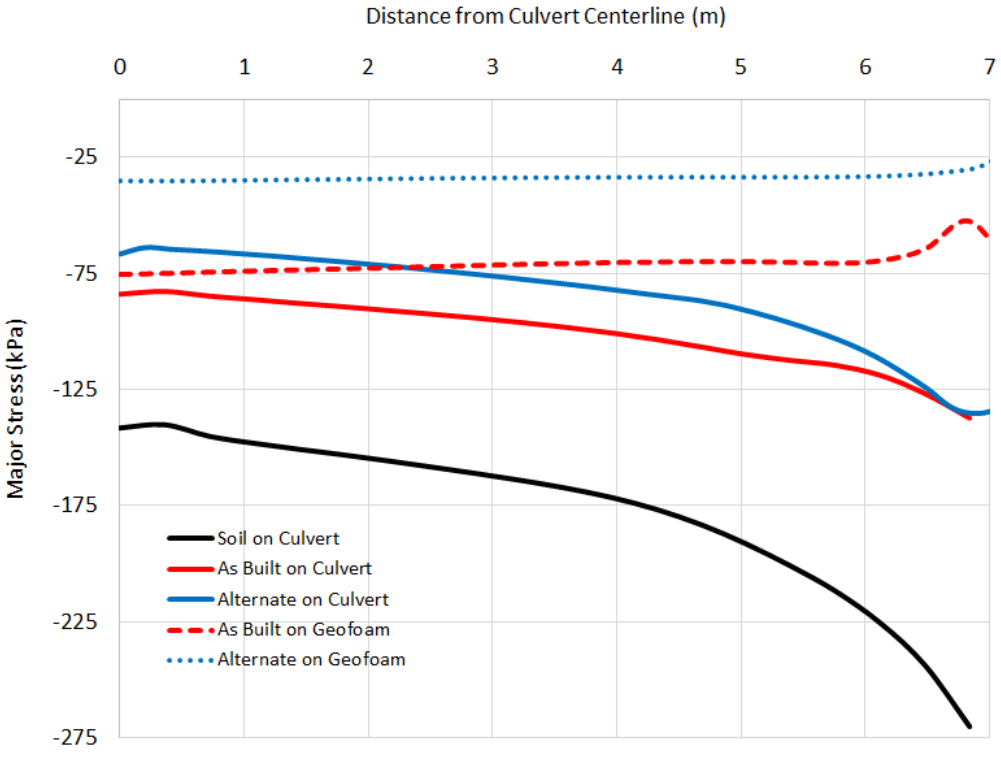

FIGURE 46 Comparison of major stresses on the culvert and the geofoam blocks.

Tables

Table 1 Summary of exhumed block densities and dimensions.

	50 Blocks Failing Density Criteria		123 Blocks Meeting Density Criteria	
	Weight (lbf)	Ave Height (in)	Weight (lbf)	Ave Height (in)
Mean	103.6	31.7	113.7	32
Min	90.5	23.3	107.5	24.2
Max	107.4	35.2	127.2	35.6

Minimum acceptable weight was 108lbf per block @ 10% below nominal. Four blocks weighed > 150lbf and were excluded.

Table 2 Summary of material properties for settlement simulations with FLAC

Material	Density (kN/m3)	Elastic Modulus (MPa)	Poisson's Ratio	Cohesion (kPa)	Friction Angle (Deg)
EPS Geofoam	0.2	6 0.55 0.375	.1	-	-
Compacted Soil	22	25	.25	1	35
Pavement	22.8	150	.30	3	38

Table 3 Unconfined compression test results for exhumed and fresh blocks.

Material	Loading	Average Density (pcf)	Average Stress (psi) @ % strain			Average Modulus (psi)
			1	5	10	
Exhumed Blocks	From Low Strain Area	1.21	5.4	15.5	17.4	5.3
	From High Strain Area	2.14	1.8	7.9	12.1	1.2
	High Strain - Rotated	2.05	6.2	22.0	25.2	6.0
Virgin Block	Initial Loading	1.16	5.7	13.7	15.5	5.6
	From Re-Loading	1.18	2.8	7.7	13.4	1.1
	Initial Rotated Axis	1.17	4.4	12.0	14.0	4.3
Typical Values EPS19		1.15	5.8	13.1	16.0	5.8

Table 4 Summary and comparison of stress conditions in the eastbound geofoam section.

	As Built Section		Revised Section	
Factor	Axial Stress (kPa)	Confining Stress (kPa)	Axial Stress (kPa)	Confining Stress
Dead Load	75	35	36	22
Mixed Density	+ 65	+ 15	-	-
Hydrostatic Pressure	+ 20	+ 20	-	-
Totals	160	70	36	22

Table 5 Summary and comparison of stress conditions on the culvert for the eastbound.

State	Maximum Vertical Stress on Center of Culvert (kPa)	Maximum Vertical Stress on Edge of Culvert (kPa)
Free Field	141	174
Negative Arching	141	270
9ft of EPS – As Built Section	84	140
Revised Section	67	135

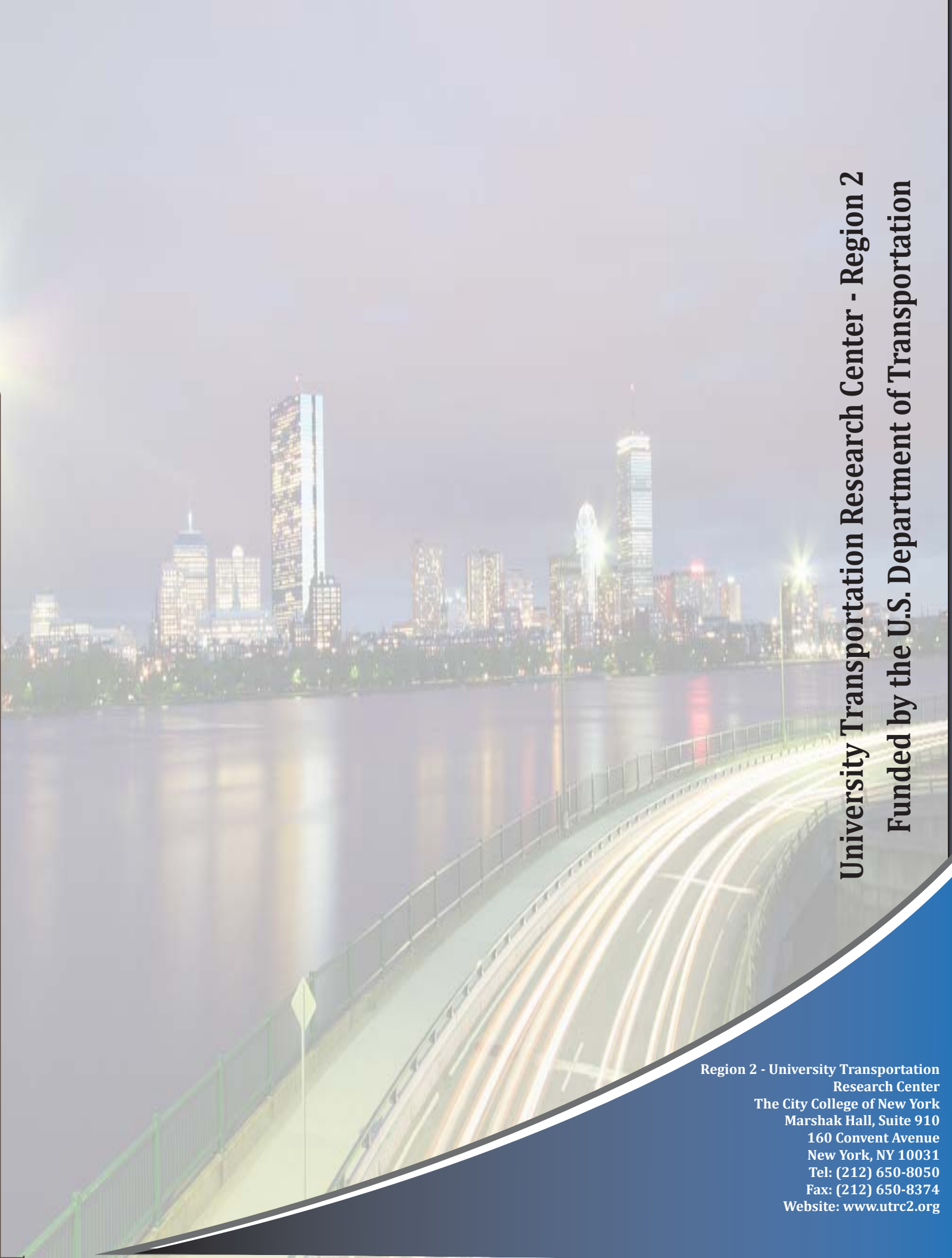

University Transportation Research Center - Region 2

Funded by the U.S. Department of Transportation

Region 2 - University Transportation
Research Center
The City College of New York
Marshak Hall, Suite 910
160 Convent Avenue
New York, NY 10031
Tel: (212) 650-8050
Fax: (212) 650-8374
Website: www.utrc2.org